Aedes anphevirus (AeAV): an insect-specific virus distributed worldwide in *Aedes aegypti* mosquitoes that has complex interplays with *Wolbachia* and dengue virus infection in cells

Rhys Parry and Sassan Asgari*

Australian Infectious Disease Research Centre, School of Biological Sciences, The University of Queensland, Brisbane, QLD 4072, Australia

Running title: Anphevirus from *Aedes aegypti*

Word count (abstract): 249

Word count (importance): 161

Word count (text): 5334

*Corresponding author: Sassan Asgari; Tel: +617 3365 2043; Fax: +617 3365 1655; s.asgari@uq.edu.au

Abstract

Insect specific viruses (ISVs) of the yellow fever mosquito *Aedes aegypti* have been demonstrated to modulate transmission of arboviruses such as dengue virus (DENV) and West Nile virus by the mosquito. The diversity and composition of the virome of *Ae. aegypti*, however, remains poorly understood. In this study, we characterised Aedes anphevirus (AeAV), a negative-sense RNA virus from the order *Mononegavirales*. AeAV identified from *Aedes* cell lines were infectious to both *Ae. aegypti* and *Aedes albopictus* cells, but not to three mammalian cell lines. To understand the incidence and genetic diversity of AeAV, we assembled 17 coding-complete and two partial genomes of AeAV from available RNA-Seq data. AeAV appears to transmit vertically and be present in laboratory colonies, wild-caught mosquitoes and cell lines worldwide. Phylogenetic analysis of AeAV strains indicates that as the *Ae. aegypti* mosquito has expanded into the Americas and Asia-Pacific, AeAV has evolved into monophyletic African, American and Asia-Pacific lineages. The endosymbiotic bacterium *Wolbachia pipientis* restricts positive-sense RNA viruses in *Ae. aegypti*. Re-analysis of a small RNA library of *Ae. aegypti* cells co-infected with AeAV and *Wolbachia* produces an abundant RNAi response consistent with persistent virus replication. We found *Wolbachia* enhances replication of AeAV when compared to a tetracycline cleared cell line, and AeAV modestly reduces DENV replication *in vitro*. The results from our study improve understanding of the diversity and evolution of the virome of *Ae. aegypti* and adds to previous evidence that shows *Wolbachia* does not restrict a range of negative strand RNA viruses.

Importance

The mosquito *Aedes aegypti* transmits a number of arthropod-borne viruses (arboviruses) such as dengue virus and Zika virus. Mosquitoes also harbour insect-specific viruses that may affect replication of pathogenic arboviruses in their body. Currently, however, there are only a handful of insect-specific viruses described from *Ae. aegypti* in the literature. Here, we characterise a novel negative strand virus, Aedes anphevirus (AeAV). Meta-analysis of *Ae. aegypti* samples showed that it is present in *Ae. aegypti* mosquitoes worldwide and

is vertically transmitted. *Wolbachia* transinfected mosquitoes are currently being used in biocontrol as they effectively block transmission of several positive sense RNA viruses in mosquitoes. Our results demonstrate that *Wolbachia* enhances the replication of AeAV and modestly reduces dengue virus replication in a cell line model. This study expands our understanding of the virome in *Ae. aegypti* as well as providing insight into the complexity of the *Wolbachia* virus restriction phenotype.

Introduction

The yellow fever mosquito *Aedes aegypti* is a vector of medically important viruses with worldwide distribution within the tropical and subtropical zones (1). *Ae. aegypti* is the principal vector of both dengue virus (DENV) and Zika virus (ZIKV) (Family: *Flaviviridae*) with estimates suggesting up to 390 million incidences of DENV infections a year (2), and approximately 400,000 cases of ZIKV during the 2015–2016 Latin American ZIKV outbreak (3).

The ability of mosquitoes to transmit viruses is determined by a complex suite of genetic and extrinsic host factors (4-6). One developing area is the contribution of insect-specific viruses (ISVs), demonstrated not to replicate in mammalian cells, in the vector competence of individual mosquitoes (7, 8). ISVs can suppress the anti-viral RNAi response as shown in Culex-Y virus (CYV) of the *Birnaviridae* family (9), or enhance the transcription of host factors; cell fusing agent virus (CFAV) (Family: *Flaviviridae*) infection of *Ae. aegypti* Aa20 cells upregulates the V-ATPase-associated factor RNASEK allowing more favourable replication of DENV (10). ISVs have also been shown to suppress or exclude replication of arboviruses; prior infection of *Aedes albopictus* C6/36 cells and *Ae. aegypti* mosquitoes with Palm Creek virus (PCV) (Family: *Flaviviridae*) has been shown to supress replication of the zoonotic West Nile virus (WNV) and Murray Valley encephalitis virus (Family: *Flaviviridae*) (11, 12). Also, it has recently been demonstrated in *Aedes* cell lines that dual infection with Phasi Charoen-like virus (Family: *Bunyaviridae*) and CFAV restricts the cells permissivity to both DENV and ZIKV infection (13).

Metagenomic and bio-surveillance strategies have proved invaluable in describing the virome diversity of wild-caught *Culicinae* mosquitoes (14, 15). To date, six ISVs have been identified and

53 characterised from wild-caught and laboratory *Ae. aegypti*; CFAV (16, 17), Phasi Charoen-like virus
54 (Family: *Bunyaviridae*) (18), Dezidougou virus from the Negevirus taxon (19), Aedes densoviruses
55 (Family: *Parvoviridae*) (20) and the unclassified Humaita-Tubiacanga virus (HTV) (21). Recently,
56 transcriptomic analysis of wild-caught *Ae. aegypti* mosquitoes from Bangkok, Thailand and Cairns,
57 Australia suggested possible infection of the mosquitoes with up to 27 insect-specific viruses, the
58 majority of which currently uncharacterized (22). This represents a narrow understanding of the
59 diversity of the circulating virome harboured by *Ae. aegypti* mosquitoes.

60 In this study, we identified and characterised a novel negative-sense RNA *Anphevirus*, putatively
61 named Aedes anphevirus (AeAV), from the order *Mononegavirales* in *Ae. aegypti* mosquitoes.
62 According to the most recent International Committee on Taxonomy of Viruses (ICTV) report (23),
63 Xīnchéng mosquito virus (XcMV), assembled as part of a metagenomic analysis of *Anopheles*
64 *sinensis* mosquitoes in Xīnchéng China, is the only member of the *Anphevirus* genus and closely
65 related to members of *Bornaviridae* and *Nyamiviridae* (24). Originally thought to only encode for four
66 ORFs, presence of a number of closely related viruses to XcMV from West African *Anopheles*
67 *gambiae* mosquitoes (15) and West Australian *Culex* mosquitoes (25) suggests that members of this
68 taxon encode for six ORFs with a genome size of approximately 12kb.

69 The endosymbiotic bacterium *Wolbachia pipientis* was first shown to restrict RNA viruses in
70 *Drosophila melanogaster* (26, 27). Transinfection of *Wolbachia* into *Ae. aegypti* restricted DENV and
71 Chikungunya virus (Family: *Togaviridae*) replication in the host (28). In *Ae. aegypti* Aag2 cells, stably
72 transinfected with a proliferative strain of *Wolbachia* (*w*MelPop-CLA), the endosymbiont restricts
73 CFAV (29), but has no effect on the negative sense Phasi Charoen-like virus (Family: *Bunyaviridae*)
74 (30). In addition to characterising AeAV, we also studied the effect of *Wolbachia* on AeAV replication
75 and co-infection of AeAV and DENV in *Ae. aegypti* cells.

76 **Results**

77 **Identification and assembly of the full Aedes anphevirus (AeAV) genome from *Wolbachia*-**
78 **infected *Aedes* cells**

79 During replication of RNA viruses in *Ae. aegypti* mosquitoes, the RNA interference (RNAi) pathway
80 cleaves viral dsRNA intermediates into 21nt short interfering RNAs (vsiRNAs) (31, 32). Using this
81 fraction of reads from RNA-Seq data, it is possible to *de novo* assemble virus genomes (21, 33).

82 The previously sequenced small RNA fraction of embryonic *Ae. aegypti* Aag2 cells and Aag2 cells
83 stably infected with *Wolbachia* (*w*MelPop-CLA strain) (34) was trimmed of adapters, filtered for 21nt
84 reads and *de novo* assembled using CLC Genomics Workbench with a minimum contig length of
85 100nt. The resulting contigs were then queried using BLASTX against a local virus protein database
86 downloaded from the National Centre for Biotechnology Information (NCBI). In the Aag2.*w*MelPop-
87 CLA assembly, four contigs between 396-1162nt were found to have amino acid similarity (E value
88 9.46E-51) to proteins from two closely related *Mononegavirales* viruses: Culex mononega-like virus
89 1 (CMLV-1) and Xīnchéng mosquito virus (XcMV); the type species for the *Anphevirus* genus. No
90 contigs from the *Wolbachia* negative *Ae. aegypti* Aag2 dataset showed any similarity to CMLV-1 or
91 XnMV.

92 Subsequent RT-PCR analysis between RNA samples from Aag2 and Aag2.*w*MelPop-CLA cell lines
93 indicated that this tentative virus was exclusive to the Aag2.*w*MelPop-CLA cell line (Fig. 1A). We
94 hypothesised that the presence of any putative virus may have been the result of contamination
95 during *Wolbachia* transinfection. The *Wolbachia* *w*MelPop-CLA strain was isolated from the *Ae.*
96 *albopictus* cell line RML-12 and transinfected into Aag2 (35) and the *Ae. albopictus* C6/36
97 (C6/36.*w*MelPop-CLA) cell lines (36). RT-PCR analysis of RNA extracted from RML-12 and C6/36
98 cells, as well as the *Ae. aegypti* cell line Aa20, showed that the putative virus was present only in
99 RML-12 cells (Fig. 1A).

100 To recover the remainder of the virus genome, transcriptome RNA-Seq data from RML-12.*w*MelPop-
101 CLA and C6/36.*w*MelPop-CLA cells were downloaded (37, 38) and *de novo* assembled with
102 automatic bubble and word sizes using CLC Genomics Workbench. BLASTN analysis of assembled
103 contigs indicated that a complete 12,940 contig from the C6/36.*w*MelPop-CLA cells and two contigs
104 (9624 and 3487nt) from RML-12.*w*MelPop-CLA were almost identical (99-100% pairwise nucleotide
105 identity) to the virus like contigs assembled from Aag2.*w*MelPop-CLA. We were then able to use this

106 reference to recover the full genomes from Aag2.*w*MelPop-CLA and RML-12.*w*MelPop-CLA
107 consensus mapping to this reference. To re-validate that AeAV was only present in Aag2.*w*MelPop-
108 CLA cells, reads from the *Wolbachia*-negative Aag2 cells were mapped to the representative
109 genome, and only four reads were identified in the data. The result from here and the RT-PCR
110 analysis above (Fig. 1A) also confirm that the virus found in the *Wolbachia* transinfected cells
111 originate from RML-12 cells in which *w*MelPop-CLA was originally transinfected and subsequently
112 transferred to other cell lines.

113 **Characterisation of Aedes anphevirus (AeAV)**

114 AeAV genomes assembled in this study were between 12,455 to 13,011 nucleotides in length with
115 a %GC content of 46.8% and encode for 7 non-overlapping ORFs (Fig. 1B). Phylogenetic analysis
116 of the RNA-dependent RNA polymerase protein places AeAV within a well-supported clade of the
117 unassigned *Anphevirus* genus, which are from the order *Mononegavirales* and closely related to
118 members of *Bornaviridae* and *Nyamiviridae* (Fig. 1C).

119 All members of *Mononegavirales* have a negative-stranded RNA genome encapsidated within the
120 capsid and the RNA polymerase complex (39). The RNA genome is used as the template by the
121 RNA polymerase complex to sequentially transcribe discrete mRNAs from subgenomic genes.
122 mRNA from each gene is capped and polyadenylated. To analyse the transcriptional activity of
123 AeAV, we used the poly-A enriched RNA-Seq libraries prepared from the Cali, Colombia laboratory
124 strain (40). Read mapping and coverage analysis of the AeAV genome showed that AeAV follows
125 the trend of reduced transcriptional activity seen in other *Mononegavirales* species (41) with
126 approximately 50% reduction between ORF1 and ORF2 but an increased transcription between
127 ORF2 and ORF3 (Fig. 1B). The reduction in transcriptional activity of AeAV genes is conserved for
128 each sequential ORF with the least transcriptional activity for ORF7/L protein, that is conserved in
129 all AeAV strains in Poly(A) enriched RNA-Seq libraries (Fig. S1).

130 ORF1 of AeAV encodes a predicted 49kDa nucleoprotein with no transmembrane domains and
131 closest pairwise amino acid identity (26%) to the nucleoprotein gene from Culex mononega-like virus
132 1 (CMLV-1) from *Culex* mosquitoes in Western Australia (25). Protein homology analysis using

133 HHPred showed that ORF1 was a likely homolog of the p40 nucleoprotein of the Borna disease virus
134 (Probability 98.66%, E- value: 7.1e-10). ORF2 encodes an 11kDa protein with two transmembrane
135 domains in the N-terminus of the protein with no similarity to any proteins within the non-redundant
136 protein database or homologs as predicted by HHPred. ORF3 and ORF4 encode putative
137 glycoproteins, 64kDa and 72kDa, respectively. ORF3 has no pairwise amino acid similarity to any
138 virus protein or homologs as per HHPred analysis. ORF4 was predicted to have a signal peptide in
139 the N-terminus followed by a heavily O- and N-linked glycosylated outside region as well as two
140 transmembrane domains in the C-terminus of the protein. ORF4 is most closely related to the
141 glycoprotein from the Gambie virus identified from West African *An. gambiae* mosquitoes with 45%
142 pairwise amino acid identity (15). Protein homology analysis predicted ORF4 to be a homolog of the
143 Human Herpesvirus 1 Envelope Glycoprotein B (Probability 99.88%, E-value 2.2e-22).

144 The presence of a Zinc-like finger (ZnF) domain in a small ORF proximal to the L protein previously
145 reported in closely related viruses (15) (Fig. 2A and B), was identified in AeAV based on sequence
146 alignment (Fig. 1B). Re-analysis of putative ORFs from CMLV-1 and CMLV-2 (25) showed the
147 presence of this GATA-like ZnF domain in both of these viruses and the genus type species XcMV
148 identified from *An. sinesis* (24) (Fig. 2C).

149 ORF6 encodes for a small 4kDa protein that has a single transmembrane domain in the C-terminus.
150 This protein was almost missed in the prediction of ORFs due to having only 37 amino acids,
151 however, it has a strong transcriptional coverage in Poly-A datasets and exists in all assembled
152 strains (Fig. 1B and Fig. S1). It was predicted to share no structural homology or amino acid identity
153 with any previously reported peptide. In addition to this, we were able to identify small
154 transmembrane domain containing proteins proximal to or overlapping with the ZnF protein in CMLV-
155 1, CMLV-2 and XcMV (Fig. 2A), suggesting that this protein may be a conserved feature of
156 anpheviruses.

157 ORF7 encodes for the 226kDa L protein, has 41% pairwise amino acid identity with the RNA
158 dependent RNA polymerase from CMLV-1. Protein domain analysis of the L protein showed the
159 highly conserved *Mononegavirales* RNA dependent RNA polymerase, mRNA capping domain and

160 a mRNA (guanine-7-) methyltransferase (G-7-MTase) domain conserved in all L proteins in
161 *Mononegavirales* (42).

162 **AeAV *cis*-regulatory elements**

163 For identification of *cis*-regulatory elements in the AeAV genome, we used MEME (Multiple Em for
164 Motif Elicitation) to search for overrepresented 5-50nt motifs (43). Using a 0-order Markov model,
165 one 32nt motif 3'-UUVCUHWUAAAAAACCCGCYAGUUASAAAUCA-5' was considered statistically
166 significant (E-value: 4.2e-010). Importantly the motif was proximal to each predicted virus gene ORF,
167 suggesting it may be a potential promoter (Fig. 3A and C). No motif was found between ORF 5 and
168 6 in AeAV suggesting that these two genes may be under the control of a single *cis*-regulatory
169 element. Interestingly, the complement of this motif appeared twice on the anti-genome suggesting
170 that it may be used in an anti-genome virus intermediate. We noticed that these motifs localised to
171 partial palindromic repeats and predicted that they may form stable secondary RNA structures. Using
172 RNAfold, we were able to visualise and predict the MFE structure 20nt upstream and downstream
173 of the motif (44). All predicted *cis*-regulatory motifs formed partial or complete stable secondary stem
174 loops and hairpins with high base-pair probabilities (Fig. 3B). The exception was predicted element
175 3, which is proximal to the second ORF; as this second gene is transcribed less than ORF3
176 irrespective of its similarity to the motif, the lack of a stable stem loop structure may be a novel
177 transcriptional regulatory mechanism. The presence of two conserved homopolymeric triplets in the
178 overrepresented motif is very similar to "slippery" -1 ribosome frame shifting (RFS) sites XXX YYY
179 Z (X=A, G, U; Y=A, U; Z=A, C, U) (45). It has been previously demonstrated that similar 'slippery'
180 sequence motifs followed by a predicted stem-loop structure is a feature of rhabdovirus gene overlap
181 regions (46). In AeAV, this feature appears in the intergenic space and is unlikely to represent
182 ribosomal frame shifting event and subsequent extension of a protein. We also searched for
183 additional slippery motifs in the AeAV genome. The genomic context for each predicted "slippery
184 motif" did not extend or produce additional ORFs.

185 **AeAV infection is widespread in *Ae. aegypti* laboratory colonies, wild-caught mosquitoes and**
186 **cell lines**

187 Taking advantage of the currently published RNA-Seq data, we performed a meta-analysis of global
188 incidence and genetic diversity of this virus. We were able to show that AeAV is ubiquitous in
189 laboratory colonies, cell lines and wild-caught *Ae. aegypti* mosquitoes. During preparation of this
190 manuscript a partial AeAV genome of 5313nt (Accession: MG012486.1) was deposited into NCBI
191 nucleotide database from a study characterising the evolution of piRNA pathways across arthropods
192 (47). Using our AeAV genome reference, we were able to complete the CDS portion of the genome
193 and also 16 additional strains of AeAV with two additional incomplete genomes (Fig. 4) (Table S1).

194 AeAV was present in colonies of *Ae. aegypti* established from eggs collected in Bakoumba, Gabon
195 (48) and also from Rabai, Kenya (designated K2, K14) as well as four mated hybrid strains (49). In
196 colonies wild caught from locations in the Americas (47), full genomes of AeAV were assembled
197 from Miami, USA , Cali, Colombia (40), and Chetumal, Mexico (50, 51) laboratory strains. Partial
198 genomes of AeAV were assembled from Cayenne and St-Georges, French Guiana (52). AeAV was
199 identified in colonies established from eggs collected in Chaiyaphum and Rayong, Thailand (49, 53)
200 as well as Jinjang, Malaysia (54). AeAV was also identified from the widely used Bora-Bora reference
201 strain from French Polynesia (55). AeAV was also present in eight pools of wild-caught *Ae. aegypti*
202 mosquitoes used for ZIKA bio-surveillance in Miami, Florida (56) as well as Nakhon Nayok, and
203 Bangkok, Thailand (18, 22).

204 In *Aedes* cell lines, AeAV was assembled from RNA-Seq data from the larval *Ae. aegypti* line CCL-
205 125 originally produced in Pune, India (57) and sequenced by the Arthropod Cell Line RNA-Seq
206 initiative, Broad Institute (broadinstitute.org). With the exception of RNA-Seq data from the three
207 *Aedes* cell lines stably infected with *Wolbachia* (RML-12.*w*MelPop-CLA, C6/36.*w*MelPop-CLA and
208 Aag2.*w*MelPopCLA), AeAV was not identified in any other available C6/36 or Aag2 RNA-Seq
209 libraries.

210 **Genetic variation and evolution of AeAV strains**

211 To assess relatedness and evolution between AeAV strains, a Maximum likelihood phylogeny
212 (PhyML) was undertaken of the CDS region of all strains with complete genomes (Fig. 5A). The

213 unrooted radial phylogenetic tree indicated three strongly supported monophyletic lineages
214 associated with the geographic origin of the sample. We have designated these lineages of AeAV
215 as African, American and Asia-Pacific (Fig. 5B).

216 In the American lineage of AeAV, all strains that are associated with *Wolbachia*-infected *Aedes* cell
217 lines (RML-12.*w*MelPop-CLA, C6/36.*w*MelPop-CLA and Aag2.*w*MelPopCLA) are almost identical
218 (99.55-99.86% identity), supporting the hypothesis that contamination of C6/36 and Aag2 cell lines
219 infected with *Wolbachia* is likely from the original RML-12 cell line. AeAV from the eight wild-caught
220 pools of *Ae. aegypti* mosquitoes from Florida, USA (56) and the laboratory colony established from
221 wild collected samples Florida (47) were almost identical (99.86% pairwise identity) with only 17nt
222 differences over the CDS region. The three African lineage strains of AeAV were slightly closer in
223 pairwise nucleotide identity to the American strains (92.65-93.15%) than the Asia/Pacific strains
224 (91.63%-91.74%). All samples that originated from Thailand form a monophyletic group and are
225 closely related to other Thai strains (99.23-99.62%).

226 We hypothesised that AeAV may have been harboured as part of the virome of *Ae. aegypti*
227 mosquitoes as *Ae. aegypti* expanded from its sub-Saharan African location into the Americas and
228 Asia-Pacific (58). Phylogenetic studies of the *Ae. aegypti* genome support the origin of *Ae. aegypti*
229 from Africa into the New World (Americas) and a subsequent secondary invasion of *Ae. aegypti*
230 *aegypti* from the New World to the Asia-Pacific region (59, 60). Comparing the evolution of the *Ae.*
231 *aegypti* nuclear genome with the evolution of AeAV indicates that the Asia-Pacific strains of AeAV
232 have not evolved from the currently circulating American strain lineage. This may indicate that the
233 virus was established independently in both the New-world Americas and also in the Asia-Pacific
234 (Fig. 5B).

235 **Anphevirus-like insertions into the *Ae. aegypti* genome**

236 The *Ae. aegypti* genome has a large repertoire of virus genes and partial viral genomes, termed
237 Endogenous Viral Elements (EVEs) (61, 62). To explore the possibility of anphevirus-like insertions
238 within the *Ae. aegypti* genome, we queried the most recent Liverpool genome (Aaegl5) with the

239 Aag2.*w*MelPop-CLA AeAV reference strain using the VectorBase BLASTN suite
240 (https://www.vectorbase.org/blast). There were numerous hits of nucleotide similarity (67-70%) of
241 500-1704nt regions dispersed throughout the *Ae. aegypti* genome. EVEs are acquired through
242 recombination with long terminal repeat (LTR) retrotransposons (62). We present one ~20kb portion
243 of Chromosome 2 of the *Ae. aegypti* genome (Fig. 6) with four anphevirus-like insertions and close
244 proximity to LTR retrotransposable fragments in unidirectional orientation. This suggests insertion of
245 viral elements through LTR retrotransposases and a long evolutionary history of challenge with
246 anphevirus-like species in *Ae. aegypti*.

247 **Aedes Anphevirus (AeAV) replicates in *Aedes* cell lines but does not replicate in three**
248 **mammalian cell lines**

249 Supernatant of Aag2.*w*MelPop-CLA cells was infectious to both *Ae. aegypti* cells (Aa20), and *Ae.*
250 *albopictus* C6/36 cells over a five-day time course through RT-qPCR analysis (Fig. 7A). Generally,
251 there was significantly more relative AeAV genome copies detected in C6/36 cells at 1 and 5 dpi
252 compared to Aa20 cells. There were also significantly more anti-genome copies of AeAV in C6/36
253 cells over the five-day time course. The higher replication of AeAV in C6/36 cells as compared to
254 Aa20 cells is not unexpected since C6/36 cells are RNAi deficient and generally RNA viruses
255 replicate more efficiently in the cells (63-65).

256 We assumed that AeAV is an insect-specific virus based on its phylogenetic position, however, to
257 test if AeAV can replicate in mammalian cells, we inoculated human hepatocellular carcinoma cells
258 (Huh-7), African green monkey cells (Vero), and baby Hamster Kidney (BSR) cells with medium from
259 AeAV-infected cells and performed RT-PCR for AeAV RNA genome abundance over a 7-day time
260 course. While AeAV RNA (most likely from the inoculum) could be detected by RT-PCR at day 1 and
261 3 after inoculation, it did not increase over time and was visibly reduced in the mammalian cells by
262 5/7 dpi (Fig. 7B). AeAV was also not detected in the *An. gambiae* cell line MOS-55 transinfected with
263 *w*MelPop-CLA from RML-12-*w*MelPop-CLA (36) sequenced by the Arthropod Cell Line RNA-Seq
264 initiative, Broad Institute (broadinstitute.org). Taken together, the results suggest that AeAV infection
265 may be restricted within the subfamily *Culicinae* or even the *Aedes* genus and is insect specific.

266 ***Wolbachia pipientis* infection in *Ae. aegypti* cells enhances AeAV replication**

267 As *Wolbachia* is being deployed in the field to reduce dengue transmission, we were interested to
268 find out if it has any effect on replication of AeAV. We extracted RNA from Aag2.*w*MelPop-CLA cells
269 and a previously tetracycline cured Aag2.*w*MelPop-CLA cell line (66), and tested the effect of
270 *Wolbachia* infection on AeAV genome and anti-genome copies. AeAV genomic RNA copies were
271 significantly greater in *Wolbachia*-infected (Aag2.*w*MelPop-CLA) cells than those in tetracycline
272 cleared (Aag2.*w*MelPop-CLA.Tet) *Ae. aegypti* cells, however, there was no statistically significant
273 difference between the relative anti-genome copies between the two cell lines (Fig. 8A).

274 To explore the host small RNA response to AeAV, clean reads from previously prepared sRNA
275 libraries from Aag2.*w*MelPop-CLA and Aag2 (34) were mapped to the AeAV genome. In the
276 cytoplasmic fraction of the Aag2.*w*MelPop-CLA sample 870,012 of 4,686,954 reads (18.56%)
277 mapped to AeAV. In the nuclear fraction 420,215 of 11,406,324 reads (3.68%) mapped to the
278 genome. In the combined Aag2 sRNA library, of 8,600,821 clean reads only four reads mapped to
279 the AeAV genome. The mapping profile of 18-31nt reads mapped from the Aag2.*w*MelPop-CLA
280 library to AeAV indicates a higher proportion 27–31nt viral derived PIWI RNAs (vpiRNAs) than the
281 21nt vsiRNAs (Fig. 8B).

282 Analysis of the profile of mapped AeAV vsiRNAs fairly ubiquitously targeted the AeAV genome and
283 anti-genome (Fig. 8C). Hotspots in the vpiRNA mapping profile appeared to target the 3'UTR and
284 ORF1 and the 5'UTR of the AeAV anti-genome (Fig. 8D). Biogenesis of vpiRNAs are independent
285 of Dicer-2 with a bias for adenosine at position 10 in the sense position and a uracil in the first
286 nucleotide of antisense polarity (67). This "ping-pong" characteristic signature was apparent in the
287 vpiRNA reads from the cell line (Fig. 8E and F).

288 **Persistent infection of AeAV in Aa20 cells modestly reduces replication of DENV-2 genomic**
289 **RNA**

290 Recently, it has been demonstrated that in *Aedes* cell lines experimentally infected with two ISVs
291 replication of DENV and ZIKV was reduced (13). To test if there was any interaction between AeAV

292 and the subsequent challenge of cells with DENV, we generated an Aa20 cell line inoculated with
293 medium from RML-12 and maintained it for three passages. Aa20 cells persistently infected with
294 AeAV were challenged with 0.1 and 1 multiplicities of infection (MOI) of DENV-2 ET-100 strain. RT-
295 qPCR analysis of DENV-2 genomic RNA showed that accumulation was on average less in AeAV
296 infected Aa20 cells as compared to the control (Fig. 9A and B). This reduction in DENV-2 genome
297 copies was statistically significant at MOI of 0.1 at both three and five days post infection. No AeAV-
298 related RT-qPCR product was detected in mock-infected Aa20 cells (data not shown). We also
299 examined the effect of DENV infection on AeAV RNA levels in the AeAV persistently infected cells.
300 RT-qPCR analysis showed no significant effect on AeAV levels between 1 and 3 days post-DENV
301 infection, however, AeAV genomic RNA levels significantly declined at 5 days-post DENV infection
302 (Fig. 9C). There was no significant difference in the results between 0.1 and 1 MOI of DENV.

303 **Evidence for vertical transmission of AeAV**

304 We were fortunate to explore the potential vertical transmission of AeAV by using RNA-Seq data of
305 uninfected and infected mated individuals from a study characterising the genetic basis of olfactory
306 preference in *Ae. aegypti* (49). Briefly, McBride and collegues used eggs from a number of *Ae.*
307 *aegypti* species in Rabai, Kenya to establish laboratory colonies for RNA-Seq analysis. We identified
308 AeAV in the domestic K2 and K14 colonies, which was seemingly absent from the other Rabai (K18,
309 K19, K27) colonies. The K27 colony was interbred with the strain K14, which we found to be AeAV
310 positive. In all the four resultant hybrid colonies, which were subjected to RNA-Seq analysis, we
311 were able to *de novo* assemble identical K14 AeAV strain genomes (Fig. 10).

312 The possibility of vertical transmission also is supported by the presence of AeAV in both RNA-Seq
313 data from the sperm of adult male mosquitoes (54) and the female reproductive tract (53).

314 **Discussion**

315 The ability of AeAV to propagate in *Ae. aegypti* and *Ae. albopictus* cell lines but not in the three
316 mammalian cell lines suggests that AeAV is most likely an ISV, although this needs to be further
317 confirmed using cell lines from other species. To the best of our knowledge, this is the first

318 comprehensive characterisation of any *Anphevirus* species within *Mononegavirales* and the first
319 *Mononegavirales* virus species within *Ae. aegypti*. Although as this manuscript was under revision,
320 the complete genome sequence of AeAV and its phylogenetic relationship with other ISVs was
321 published in a short communication (68). While we have demonstrated that AeAV is spread
322 worldwide in *Ae. aegypti* mosquitoes, we have limited understanding as to how prevalent AeAV is in
323 individual mosquitoes in wild populations, its tissue tropism, or potential impacts on the host.
324 Although it is likely that AeAV is maintained in wild populations of *Ae. aegypti* mosquitoes through
325 vertical transmission, it is possible that AeAV could be maintained though venereal transmission as
326 we were able to identify the whole AeAV genome from a dataset prepared from the sperm of adult
327 male *Ae. aegypti* mosquitoes (54).

328 To our knowledge, the oldest continually maintained colony of laboratory mosquitoes with AeAV
329 present comes from Jinjang, Malaysia, which was established from wild-collected samples from as
330 early as 1975 (54). This suggests vertical transmission rates of AeAV are high or a high incidence
331 of AeAV within the colony. In comparison, in both French Guiana colonies, we were unable to recover
332 the complete genomes from these strains. It is unlikely that this is due to insertion of AeAV into the
333 nuclear *Ae. aegypti* genome as numerous reads mapped to the ORF7/L region of the reference
334 strain; however, there was not enough coverage to reach consensus of the full genome. As these
335 libraries were prepared from homogenates of mosquitoes, it seems likely that the incidence of
336 infection within these colonies may be lower; however, further analysis would have to be conducted.

337 In our analysis, AeAV was not detected in any of the widely used Liverpool (LVP) and
338 Rockefeller/UGAL, as well as derived "white eye mutant" strains of *Ae. aegypti.* Analysis of published
339 ncRNA-Seq data from Australian Townsville and Cairns colonies of wild-caught Australian
340 mosquitoes (69, 70) suggests that there is no RNAi response or presence of AeAV in these
341 mosquitoes. Evidence from this study and others suggests that widely used laboratory strains of *Ae.*
342 *aegypti* harbour a diverse and heterogeneous virome composition and may contribute to the variable
343 vector competence between these colonies.

344 In our analysis, the geographic origin of the RNA-Seq samples matched the resulting phylogenetic
345 relationship of each strain. The presence of AeAV in the *Ae. albopictus* cell line RML-12, presumably
346 the origin of the AeAV contamination in other *Aedes* cell lines transinfected with adapted *w*MelPop
347 strain, was the only *Ae. albopictus* sample in our analysis. During our analysis, we queried all of the
348 266 currently available *Ae. albopictus* RNA-Seq datasets (TaxonID: 7160) uploaded to the SRA,
349 none of which indicated presence of AeAV. We hypothesise that AeAV from RML-12 is likely due to
350 contamination as the cell line is often mischaracterised as originating from *Ae. aegypti* (71, 72). In
351 many laboratories that study arbovirus interactions, more than one *Aedes* cell line is maintained. As
352 the RML-12 AeAV strain is genetically placed within the American lineage, and the namesake of the
353 cell line, Rocky Mountain Laboratories, (71) located in Montana, USA suggests possible
354 contamination from domestic *Ae. aegypti* mosquito samples. While no other *Ae. albopictus* RNA-
355 Seq data were positive for AeAV in this study, we cannot rule out the possibility that AeAV could
356 exist in American populations of *Ae. albopictus*. *Ae. aegypti* and *Ae. albopictus* co-exist in North
357 America and compete for larval habitats of discarded tires and other artificial containers (73).

358 RNAi response is commonly observed in mosquitoes against RNA viruses. This response includes
359 miRNA, siRNA and piRNA pathways (74, 75). Similarly, we found a large number of 21nt vsiRNAs
360 produced against AeAV in infected cells that were evenly mapped to both sense and antisense
361 strands, indicating that dsRNA intermediates produced during replication must be the target of the
362 host cell RNAi response. In addition, a large number of vpiRNAs were found mapped to the 5'UTR,
363 ORF1 and the 3'UTR of the AeAV genome. These vpiRNAs had the typical ping-pong signature (U_1-
364 A_{10}) of secondary piRNAs. This signature has also been found in vpiRNAs produced during
365 alphavirus (76) and bunyavirus (63, 77) infections, but not in vpiRNA-like small RNAs in most
366 flaviviruses, such as DENV (78), ZIKV (79, 80) and an insect-specific flavivirus (81). We found a
367 higher proportion of small RNAs from Aag2-*w*MelPop-CLA cells that mapped to AeAV are vpiRNAs
368 (about 50%) as compared to less than 10% vsiRNAs. Literature suggests that when the siRNA
369 pathway is compromised more vpiRNAs are produced. This has been shown in RNAi deficient C6/36
370 cells when infected with Sindbis virus, Rift Valley fever virus or La Crosse virus (63-65). The RNA-

371 Seq data from C6/36.*w*MelPop-CLA cells were for long transcripts rather than small RNAs, therefore
372 we were not able to confirm if in those cells there are higher proportion of vpiRNAs than vsiRNAs.
373 The over-representation of vpiRNAs in respect to vsiRNAs has also been demonstrated in negative-
374 sense *Bunyavirales* members PCLV and RVFV (30, 65) in Aag2 cells for all segments of the genome.
375 It remains to be seen however if the higher vpiRNA to vsiRNA ratio in Aag2.*w*MelPop-CLA could be
376 due to suppression of the siRNA pathway by AeAV, or alternatively, *Wolbachia* may have an effect
377 on the siRNA pathway. It seems however more likely that as negative sense RNA viruses produce
378 less dsRNA replicative intermediates, these could be simply less targeted by the siRNA pathway
379 and are unable to be resolved by sRNA profiling. These possibilities require further investigations,
380 and it remains to determine the role of the vpiRNAs in AeAV replication or host anti-viral response.

381 The effects of *Wolbachia* on virus restriction are variable and depend on *Wolbachia* strain, virus
382 family and transinfected host (82). *Wolbachia* was shown to enhance AeAV replication in *Ae. aegypti*
383 cells in this study. Recent studies have demonstrated that *Wolbachia* has no effect on multi-
384 segmented negative-sense RNA viruses; for example, Phasi Charoen-like virus (PCLV) (Family:
385 *Bunyaviridae*) in *w*MelPop-CLA strain infected Aag2 cells (30), La Crosse virus (Family:
386 *Bunyaviridae*) and vesicular stomatitis virus (Family: *Rhabdoviridae*), which is in the same order as
387 AeAV, in *w*Stri strain in *Ae. albopictus* C710 cell line (83), and the Rift Valley fever virus (RVFV)
388 (Family: *Phenuiviridae*), in *Culex tarsalis* mosquitoes transinfected with a somatic *Wolbachia* (strain
389 *w*AlbB) had no effect on RVFV infection or dissemination (84), respectively. RVFV and PCLV belong
390 to the *Bunyavirales* order and AeAV belongs to *Mononegavirales*, distinct orders of negative strand
391 RNA viruses. All three viruses have conserved features that may provide insight into how they might
392 be protected from restriction by *Wolbachia*. The genome of all negative-sense ssRNA viruses is both
393 encapsidated within the nucleoprotein (85, 86) and is attached to RNA dependent RNA polymerase
394 within the virion (87). The RNA dependent polymerase complex carries out both transcription of virus
395 genes and replication of the genome.

396 *Wolbachia* has been shown to restrict a number of positive-sense RNA virus species from the
397 *Togaviridae* and *Flaviviridae* families (82). After fusion and entry into the host cell, the genomes of

398 *Togaviridae* and *Flaviviridae* species are released into the cytoplasm and translated directly into
399 polypeptide protein(s). These polypeptide proteins are processed by viral and cellular proteases to
400 generate the mature structural and non-structural proteins which are then used to replicate the
401 genome (88). While the exact mechanism for RNA virus restriction in *Wolbachia*-infected insects has
402 remained elusive, it has been shown that restriction of RNA viruses by *Wolbachia* happens early in
403 infection (89, 90). In the *Ae. albopictus* cell line C710 stably infected with *w*Stri, the polypeptide of
404 ZIKV is not produced as determined by immunoblot at one day post-infection (90). Additionally,
405 *Wolbachia* exploits host innate immunity to establish a symbiotic relationship with *Ae. aegypti* (91).
406 Perhaps the combination of protection of the RNA nucleocapsid genome or genome segments when
407 released in the cytoplasm or activity of the RNA-dependent RNA polymerase may aid in evasion of
408 host immune response enhanced by *Wolbachia* or *Wolbachia* effector molecules (92). However, a
409 recent study suggested increases in infection of *Ae. aegypti* mosquitoes by insect-specific
410 flaviviruses when they harbour *Wolbachia w*Mel strain (93).

411 The ability of AeAV to modestly reduce DENV-2 genomic RNA in a persistently infected cell line was
412 unexpected. While it has previously been shown that members of the same virus family can provide
413 super exclusion of additional viruses (12, 94), little work has been undertaken to look at cross viral
414 family exclusion effects. Our results showed that less DENV replication occured in the presence of
415 AeAV, with the difference particularly significant at lower MOI. If this suppressive effect also occurs
416 in mosquitoes, enhancement of AeAV in *Ae. aegypti* mosquitoes infected with *Wolbachia* may be
417 beneficial in terms of DENV suppression.

418 As *Ae. aegypti* is perhaps the most important vector of arboviruses worldwide, further work should
419 be undertaken in understanding and characterising the virome of this mosquito and effects on
420 mosquito life-history traits. Our findings provide new insights into the evolution and genetic diversity
421 of AeAV across a wide geographic range as well as providing valuable insights into the virus features
422 and families restricted by *Wolbachia* in mosquito hosts and its effects on arboviruses they transmit.

423 **Materials and Methods**

424 **Cell lines maintenance and experimental infection with AeAV**

425 *Ae. aegypti* cell line (Aag2) stably infected with *Wolbachia* (denoted Aag2.*w*MelPop-CLA) as
426 previously described for the C6/36.*w*MelPop-CLA (35), with its previously generated tetracycline-
427 treated line (66), and both *Ae. albopictus* C6/36 cell line (57) and RML-12 cell lines were maintained
428 in 1:1 Mitsuhashi-Maramorosch and Schneider's insect medium (Invitrogen) supplemented with 10%
429 Fetal Bovine Serum (FBS, Bovogen Biologicals). Aa20 cells established from *Ae. aegypti* larvae (95)
430 were maintained in Leibovitz's L15 medium supplemented with 10% FBS (France – Biowest) and
431 10% Tryptose phosphate broth at 27°C. African green monkey cells (Vero) were maintained in Opti-
432 MEM I Reduced-Serum Medium supplemented with 2% FBS and 10 mL/L Penicillin-Streptomycin
433 (Sigma-Aldrich). Human hepatocellular carcinoma cells (Huh-7) were maintained in Opti-MEM I
434 Reduced-Serum Medium supplemented with 5% FBS and 10 mL/L Penicillin-Streptomycin (Sigma-
435 Aldrich). BSR cells (a clone of Baby Hamster Kidney-21) were maintained in Dulbecco's Modified
436 Eagle Medium (Gibco), 2% FBS and 10 mL/L Penicillin-Streptomycin (Sigma-Aldrich). All
437 mammalian cells were kept at 37°C with 5%CO_2.

438 For experimental infection of cells, 10^6 cells of *Aedes* or mammalian cells were seeded in a 12-well
439 plate. Subsequently, supernatant from Aag2.*w*MelPop-CLA cells was collected, centrifuged at
440 2150×g for 5 min to remove cells and debris, and used as an AeAV inoculation source. One Aa20
441 cell line was experimentally inoculated with RML-12 cell supernatant and kept as a persistently
442 infected AeAV cell line. Cells were collected at 1, 3 and 5 days post-inoculation for *Aedes* cell lines
443 for RT-qPCR analysis and 1, 3, 5 and 7 days for mammalian cell lines for RT-PCR analysis.

444 **Aedes anphevirus (AeAV) and dengue virus (DENV-2) interaction assay**

445 The third passage of Aa20 cells persistently infected with AeAV (denoted $Aa20_{AeAV}$) and Aa20 mock
446 were seeded at the density of 3×10^5 cells in 12-well plates overnight. Cells were then infected with
447 the East Timor (ET-100) DENV-2 strain at a multiplicity of infection (MOI) of 0.1 and 1, cells were
448 rocked for an hour at room temperature and supernatant was discarded and replaced with fresh
449 medium. Cells were collected at 0, 1, 3 and 5dpi after infection with mock collected at 5 dpi. Cells

450 were subjected to RNA extraction to quantify the DENV-2 genomic RNA levels by RT-qPCR as
451 described below.

452 **Assembly and identification of AeAV strains from RNA-Seq data**

453 For detection of AeAV in previously published RNA-Seq data, we used the assembled RML-12 AeAV
454 genome as a BLASTN query for all available *Ae. aegypti* (taxonID: 7159) RNA-Seq data within the
455 Sequence Read Archive (SRA) on NCBI. SRA run files with positive hits of 90-100% identity and an
456 E value <2E-30 were downloaded and converted to fastq using the NCBI SRA toolkit
457 https://www.ncbi.nlm.nih.gov/sra/docs/toolkitsoft/ for further analysis. FastQC
458 (https://www.bioinformatics.babraham.ac.uk/projects/fastqc/) was used for quality checking of fastq
459 files and adapter identification. Fastq files were then imported into CLC Genomics Workbench
460 (10.1.1) and were adapter and quality trimmed (<0.02; equivalent Phred quality score of 17,
461 ambiguous nucleotides: 2).

462 Two strategies were used to assemble strains of AeAV; fastq files from the same source of *Ae.*
463 *aegypti* were pooled and *de novo* assembled using the CLC Genomics Workbench assembly
464 program with automatic bubble and word sizes. This was sufficient to assemble the full coding
465 sequences (CDS) of most strains of AeAV. Table S1 contains *de novo* assembly statistics from each
466 dataset used.

467 If *de novo* assembly did not produce the complete AeAV genome, to complete further sections of
468 the AeAV genome clean reads were mapped to the C6/36.*w*MelPop-CLA strain of AeAV with
469 stringent alignment criteria (Match score:1 Mismatch cost:2 length fraction 0.89 and similarity fraction
470 0.89) to exclude false-positive mapping that derives from Endogenous Viral Elements (EVEs). To
471 confirm accuracy of assembly, the largest contigs of consensus mapping were extracted and then
472 used as a reference for re-mapping and manually checked. Final sequences of the virus genomes
473 were obtained through the majority consensus of the mapping assembly and were given Coding
474 Complete (CC) or Standard Draft (SD) genome quality ratings (96).

475 **RNA isolation, strand specific cDNA synthesis and RT-qPCR**

476 Total RNA was extracted from mosquito cells using QIAzol Lysis Reagent (QIAGEN) and treated
477 with Turbo DNase (Thermo Fisher Scientific) as per manufacturer's instructions. RNA quality and
478 quantity were evaluated using a BioTek Epoch Microspot Plate Spectrophotometer. For the
479 production of AeAV genome and anti-genome cDNA, two cDNA reactions were generated using
480 600ng of RNA and SuperScript III Reverse Transcriptase (Thermo Fisher Scientific). The genome
481 cDNA strand was synthesised using a forward primer to AeAV (AeAVGenome-RT 5'-
482 AGACTTCTAAGCCTGCCCACA -3'), and the AeAV anti-genome cDNA strand was synthesised
483 using a reverse orientation primer (AeAVAntiGenome-RT 5'- ACACTTGCCATGTGCTCAG -3').
484 *Aedes* Ribosomal protein subunit 17 (RPS17) primers (*Ae. aegypti*: AeRPS17-qR 5'-
485 GGACACTTCGGGCACGTAGT-3' and *Ae. albopictus* AalRPS17q-R 5'-
486 ACGTAGTTGTCTCTCTGCGCTC -3') were used for reference gene cDNA synthesis. Following RT,
487 qPCR with AeAV primers (AeAV-qF 5'-GACAATCGCATTGGCTGCAT-3' and AeAV-qR 5'-
488 CCCGAGACAATCGGCTTCTT - 3') as well as primer pairs for the RPS17 genes (*Ae. aegypti:*
489 AeRPS17-qF 5'- CACTCCGAGGTCCGTGGTAT -3' and *Ae. albopictus:* AalRPS17-qF 5'-
490 CGCTGGTTTCGTGACACATC -3') were undertaken. RPS17 was used for normalizing data as
491 described previously in *Ae. aegypti* cells (97).

492 For quantitation of DENV-2 genome copies in Aa20 cells, two SuperScript III reverse transcription
493 (Thermo Fisher Scientific) reactions with 1000ng of RNA were prepared. For DENV-2 genome
494 copies reaction, the reverse primer (DENV2-qR 5'- CAAGGCTAACGCATCAGTCA -3') and in a
495 separate cDNA synthesis reaction the *Ae. aegypti* RPS17 primers as described above.
496 Subsequently, qPCR for DENV-2 was carried out using the DENV-2 primer pair (DENV2-qF 5'-
497 GGTATGGTGGGCGCTACTA -3' and DENV2-qR), and RPS17 was used as a normalising control
498 as also described above.

499 Each time-point for experimental infection was run with three biological replicates and two technical
500 replicates. Platinum SYBR Green Mix (Invitrogen) was used for qPCR with 20ng of RT products in
501 a Rotor-Gene thermal cycler (QIAGEN) as described above. The relative abundance of AeAV RNA

502 and DENV-2 to the host reference gene was determined by qGENE software using the $\Delta\Delta C_t$ method
503 and analyzed using GraphPad Prism.

504 To test for the replication of AeAV in mammalian cells, 1000ng of total RNA extracted from the cells
505 was extracted and used for first stand synthesis with SuperScript III reverse transcriptase with the
506 AeAVGenome-RT primer. qPCR was subsequently carried out using AeAVGenome-RT primer and
507 the qPCR primer AeAVqR2 5'-ATGAAAGTATGGATACACACCGCG-3'. Products were then
508 visualised on a 1% agarose gel.

509 **Virus genome annotation**

510 Potential ORFs of AeAV were analysed using NCBI Open Reading Frame Finder
511 (https://www.ncbi.nlm.nih.gov/orffinder/) with a minimal ORF length of 150. ORFs were cross
512 referenced with mapping from Poly(A) enriched transcriptomes (Fig. S1) to reduce false positive
513 identification of ORFs. For determination of putative domains in AeAV, ORFs were translated and
514 searched against the Conserved Domain Search Service (CD Search)
515 (https://www.ncbi.nlm.nih.gov/Structure/cdd/wrpsb.cgi). For protein homology detection, we used
516 the HHPred webserver on translated AeAV ORFs (98).

517 To best discriminate N-terminus transmembrane domains from signal peptides, we used the
518 consensus TOPCONS webserver (99). Glycosylation sites were predicted by the NetNGlyc 1.0/
519 NetOGlyc 4.0 Server (http://www.cbs.dtu.dk/services/).

520 **Phylogenetic analysis**

521 For placement of AeAV within the order *Mononegavirales*, ClustalW was used on CLC Genomics
522 Workbench to align amino acid sequences of 30 L proteins of the most closely related
523 *Mononegavirales* species as determined by BLASTp of the NCBI non-redundant database. A
524 Maximum likelihood phylogeny (PhyML) was constructed using the Whelan and Goldman (WAG)
525 amino acid substitution model with 1000 bootstraps. Accession numbers and associated hosts used
526 to produce the phylogenetic tree are available in Table S1.

527 To determine relatedness between different strains of AeAV, genomes that were coding complete
528 and greater than 30x coverage were trimmed of 3'UTR and 5'UTR regions and aligned using the
529 ClustalW algorithm on CLC Genomics Workbench. A Maximum likelihood phylogeny (PhyML) was
530 constructed. A Hierarchical likelihood ratio test (hLRT) with a confidence level of 0.01 suggested that
531 the General Time Reversible (GTR) +G (Rate variation 4 categories) and +T (topology variation)
532 nucleotide substitution model was the most appropriate. 1000 bootstrap replicates were performed
533 with 95% bootstrap branching support cut-off.

534 **Statistical analysis**

535 Statistical analysis Unpaired t-test was used to compare differences between two individual groups,
536 while One-way ANOVA with Tukey's post-hoc test was carried out to compare differences between
537 more than two groups. Data that did not pass the normality test were re-analysed by the non-
538 parametric Wilcoxon test indicated in their relevant figure legends.

539 **Accession numbers**

540 All the complete and incomplete virus genome sequences generated in this study have been
541 deposited in Genbank under the accession numbers (MH037149 and MH430648-MH430666).

542 **Acknowledgements**

543 This project was funded by the Australian Research Council grant (ARC, DP150101782) to SA and
544 University of Queensland scholarship to RP. For the supply of the DENV-2 (ET-100) strain, we thank
545 Dr Daniel Watterson and Professor Paul Young from the University of Queensland. We thank Dr
546 Daniel Watterson and Dr Jody Hobson-Peters for providing Huh-7 and BSR cells, respectively. The
547 authors would like to thank the technical assistance of Dr Sultan Asad, Dr Kayvan Etebari and Hugo
548 Perdomo Contreras, as well as current and former members of the Asgari lab for their fruitful
549 conversations.

550 **References**

551 1. **Shriram AN, Sivan A, Sugunan AP.** 2017. Spatial distribution of *Aedes aegypti* and
552 *Aedes albopictus* in relation to geo-ecological features in South Andaman, Andaman
553 and Nicobar Islands, India. Bull Entomol Res **3:**166-174.

2. **Bhatt S, Gething PW, Brady OJ, Messina JP, Farlow AW, Moyes CL, Drake JM, Brownstein JS, Hoen AG, Sankoh O, Myers MF, George DB, Jaenisch T, Wint GR, Simmons CP, Scott TW, Farrar JJ, Hay SI.** 2013. The global distribution and burden of dengue. Nature **496:**504-507.
3. **ECDC.** 2015. Rapid risk assessment: Zika virus epidemic in the Americas: potential association with microcephaly and Guillain-Barré syndrome. European Centre for Disease Prevention and Control S, https://ecdc.europa.eu/sites/portal/files/media/en/publications/Publications/zika-virus-americas-association-with-microcephaly-rapid-risk-assessment.pdf.
4. **Tabachnick WJ.** 2013. Nature, nurture and evolution of intra-species variation in mosquito arbovirus transmission competence. Int J Environ Res Public Health **10:**249-277.
5. **Weiss B, Aksoy S.** 2011. Microbiome influences on insect host vector competence. Trends Parasitol **27:**514-522.
6. **Beerntsen BT, James AA, Christensen BM.** 2000. Genetics of mosquito vector competence. Microbiol Mol Biol Rev **64:**115-137.
7. **Hall RA, Bielefeldt-Ohmann H, McLean BJ, O'Brien CA, Colmant AM, Piyasena TB, Harrison JJ, Newton ND, Barnard RT, Prow NA, Deerain JM, Mah MG, Hobson-Peters J.** 2016. Commensal viruses, transmission, and interaction with arboviral pathogens. Evol Bioinform Online **12:**35-44.
8. **Blitvich BJ, Firth AE.** 2015. Insect-specific flaviviruses: a systematic review of their discovery, host range, mode of transmission, superinfection exclusion potential and genomic organization. Viruses **7:**1927-1959.
9. **van Cleef KW, van Mierlo JT, Miesen P, Overheul GJ, Fros JJ, Schuster S, Marklewitz M, Pijlman GP, Junglen S, van Rij RP.** 2014. Mosquito and Drosophila entomobirnaviruses suppress dsRNA- and siRNA-induced RNAi. Nucleic Acids Res **42:**8732-8744.
10. **Zhang G, Asad S, Khromykh AA, Asgari S.** 2017. Cell fusing agent virus and dengue virus mutually interact in Aedes aegypti cell lines. Sci Rep **7:**6935.
11. **Hobson-Peters J, Yam AW, Lu JW, Setoh YX, May FJ, Kurucz N, Walsh S, Prow NA, Davis SS, Weir R, Melville L, Hunt N, Webb RI, Blitvich BJ, Whelan P, Hall RA.** 2013. A new insect-specific flavivirus from northern Australia suppresses replication of West Nile virus and Murray Valley encephalitis virus in co-infected mosquito cells. PLoS One **8:**e56534.
12. **Hall-Mendelin S, McLean BJ, Bielefeldt-Ohmann H, Hobson-Peters J, Hall RA, van den Hurk AF.** 2016. The insect-specific Palm Creek virus modulates West Nile virus infection in and transmission by Australian mosquitoes. Parasit Vectors **9:**414.
13. **Schultz MJ, Frydman HM, Connor JH.** 2018. Dual Insect specific virus infection limits Arbovirus replication in *Aedes* mosquito cells. Virology **518:**406-413.
14. **Chandler JA, Liu RM, Bennett SN.** 2015. RNA shotgun metagenomic sequencing of northern California (USA) mosquitoes uncovers viruses, bacteria, and fungi. Front Microbiol **6:**185.
15. **Fauver JR, Grubaugh ND, Krajacich BJ, Weger-Lucarelli J, Lakin SM, Fakoli LS, 3rd, Bolay FK, Diclaro JW, 2nd, Dabire KR, Foy BD, Brackney DE, Ebel GD, Stenglein MD.** 2016. West African *Anopheles gambiae* mosquitoes harbor a taxonomically diverse virome including new insect-specific flaviviruses, mononegaviruses, and totiviruses. Virology **498:**288-299.
16. **Bolling BG, Vasilakis N, Guzman H, Widen SG, Wood TG, Popov VL, Thangamani S, Tesh RB.** 2015. Insect-specific viruses detected in laboratory

603 mosquito colonies and their potential implications for experiments evaluating
604 arbovirus vector competence. Am J Trop Med Hyg **92:**422-428.
605 17. **Cook S, Bennett SN, Holmes EC, De Chesse R, Moureau G, de Lamballerie X.**
606 2006. Isolation of a new strain of the flavivirus cell fusing agent virus in a natural
607 mosquito population from Puerto Rico. J Gen Virol **87:**735-748.
608 18. **Chandler JA, Thongsripong P, Green A, Kittayapong P, Wilcox BA, Schroth GP,**
609 **Kapan DD, Bennett SN.** 2014. Metagenomic shotgun sequencing of a Bunyavirus in
610 wild-caught *Aedes aegypti* from Thailand informs the evolutionary and genomic
611 history of the Phleboviruses. Virology **464-465:**312-319.
612 19. **Vasilakis N, Forrester NL, Palacios G, Nasar F, Savji N, Rossi SL, Guzman H,**
613 **Wood TG, Popov V, Gorchakov R, Gonzalez AV, Haddow AD, Watts DM, da**
614 **Rosa AP, Weaver SC, Lipkin WI, Tesh RB.** 2013. Negevirus: a proposed new taxon
615 of insect-specific viruses with wide geographic distribution. J Virol **87:**2475-2488.
616 20. **Kittayapong P, Baisley KJ, O'Neill SL.** 1999. A mosquito densovirus infecting
617 Aedes aegypti and Aedes albopictus from Thailand. Am J Trop Med Hyg **61:**612-617.
618 21. **Aguiar ER, Olmo RP, Paro S, Ferreira FV, de Faria IJ, Todjro YM, Lobo FP, Kroon**
619 **EG, Meignin C, Gatherer D, Imler JL, Marques JT.** 2015. Sequence-independent
620 characterization of viruses based on the pattern of viral small RNAs produced by the
621 host. Nucleic Acids Res **43:**6191-6206.
622 22. **Zakrzewski M, Rasic G, Darbro J, Krause L, Poo YS, Filipovic I, Parry R, Asgari**
623 **S, Devine G, Suhrbier A.** 2018. Mapping the virome in wild-caught Aedes aegypti
624 from Cairns and Bangkok. Sci Rep **16:**4690.
625 23. **Amarasinghe GK, Bao Y, Basler CF, Bavari S, Beer M, Bejerman N, Blasdell KR,**
626 **Bochnowski A, Briese T, Bukreyev A, Calisher CH, Chandran K, Collins PL,**
627 **Dietzgen RG, Dolnik O, Durrwald R, Dye JM, Easton AJ, Ebihara H, Fang Q,**
628 **Formenty P, Fouchier RAM, Ghedin E, Harding RM, Hewson R, Higgins CM,**
629 **Hong J, Horie M, James AP, Jiang D, Kobinger GP, Kondo H, Kurath G, Lamb**
630 **RA, Lee B, Leroy EM, Li M, Maisner A, Muhlberger E, Netesov SV, Nowotny N,**
631 **Patterson JL, Payne SL, Paweska JT, Pearson MN, Randall RE, Revill PA, Rima**
632 **BK, Rota P, Rubbenstroth D, Schwemmle M, Smither SJ, Song Q, Stone DM,**
633 **Takada A, Terregino C, Tesh RB, Tomonaga K, Tordo N, Towner JS, Vasilakis**
634 **N, Volchkov VE, Wahl-Jensen V, Walker PJ, Wang B, Wang D, Wang F, Wang**
635 **LF, Werren JH, Whitfield AE, Yan Z, Ye G, Kuhn JH.** 2017. Taxonomy of the order
636 Mononegavirales: update 2017. Arch Virol **162:**2493-2504.
637 24. **Li CX, Shi M, Tian JH, Lin XD, Kang YJ, Chen LJ, Qin XC, Xu J, Holmes EC,**
638 **Zhang YZ.** 2015. Unprecedented genomic diversity of RNA viruses in arthropods
639 reveals the ancestry of negative-sense RNA viruses. eLife **4:**e05378.
640 25. **Shi M, Neville P, Nicholson J, Eden JS, Imrie A, Holmes EC.** 2017. High-resolution
641 metatranscriptomics reveals the ecological dynamics of mosquito-associated RNA
642 viruses in Western Australia. J Virol **91:**e00680-00617.
643 26. **Hedges LM, Brownlie JC, O'Neill SL, Johnson KN.** 2008. *Wolbachia* and virus
644 protection in insects. Science **322:**702.
645 27. **Teixeira L, Ferreira A, Ashburner M.** 2008. The bacterial symbiont *Wolbachia*
646 induces resistance to RNA viral infections in *Drosophila melanogaster*. PLoS Biol
647 **6:**e2.
648 28. **Moreira LA, Iturbe-Ormaetxe I, Jeffery JA, Lu G, Pyke AT, Hedges LM, Rocha**
649 **BC, Hall-Mendelin S, Day A, Riegler M, Hugo LE, Johnson KN, Kay BH, McGraw**
650 **EA, van den Hurk AF, Ryan PA, O'Neill SL.** 2009. A *Wolbachia* symbiont in *Aedes*
651 *aegypti* limits infection with dengue, Chikungunya, and *Plasmodium*. Cell **139:**1268-
652 1278.

29. **Zhang G, Etebari K, Asgari S.** 2016. *Wolbachia* suppresses cell fusing agent virus in mosquito cells. J Gen Virol **97:**3427-3432.
30. **Schnettler E, Sreenu VB, Mottram T, McFarlane M.** 2016. *Wolbachia* restricts insect-specific flavivirus infection in *Aedes aegypti* cells. J Gen Virol **97:**3024-3029.
31. **Sabin LR, Zheng Q, Thekkat P, Yang J, Hannon GJ, Gregory BD, Tudor M, Cherry S.** 2013. Dicer-2 processes diverse viral RNA species. PLoS One **8:**e55458.
32. **Sanchez-Vargas I, Scott JC, Poole-Smith BK, Franz AW, Barbosa-Solomieu V, Wilusz J, Olson KE, Blair CD.** 2009. Dengue virus type 2 infections of Aedes aegypti are modulated by the mosquito's RNA interference pathway. PLoS Pathog **5:**e1000299.
33. **Wu Q, Luo Y, Lu R, Lau N, Lai EC, Li WX, Ding SW.** 2010. Virus discovery by deep sequencing and assembly of virus-derived small silencing RNAs. Proc Natl Acad Sci U S A **107:**1606-1611.
34. **Mayoral JG, Etebari K, Hussain M, Khromykh AA, Asgari S.** 2014. Wolbachia infection modifies the profile, shuttling and structure of microRNAs in a mosquito cell line. PLoS One **9:**e96107.
35. **Frentiu FD, Robinson J, Young PR, McGraw EA, O'Neill SA.** 2010. *Wolbachia*-mediated resistance to Dengue virus infection and death at the cellular level. PLoS One **5:**e13398.
36. **McMeniman CJ, Lane AM, Fong AW, Voronin DA, Iturbe-Ormaetxe I, Yamada R, McGraw EA, O'Neill SL.** 2008. Host adaptation of a *Wolbachia* strain after long-term serial passage in mosquito cell lines. Appl Environ Microbiol **74:**6963-6969.
37. **Darby AC, Gill AC, Armstrong SD, Hartley CS, Xia D, Wastling JM, Makepeace BL.** 2014. Integrated transcriptomic and proteomic analysis of the global response of *Wolbachia* to doxycycline-induced stress. ISME J **8:**925-937.
38. **Woolfit M, Algama M, Keith JM, McGraw EA, Popovici J.** 2015. Discovery of putative small non-coding RNAs from the obligate intracellular bacterium *Wolbachia pipientis*. PLoS One **10:**e0118595.
39. **Green TJ, Cox R, Tsao J, Rowse M, Qiu S, Luo M.** 2014. Common mechanism for RNA encapsidation by negative-strand RNA viruses. J Virol **88:**3766-3775.
40. **Baron OL, Ursic-Bedoya RJ, Lowenberger CA, Ocampo CB.** 2010. Differential gene expression from midguts of refractory and susceptible lines of the mosquito, *Aedes aegypti*, infected with Dengue-2 virus. J Insect Sci **10:**41.
41. **Iverson LE, Rose JK.** 1981. Localized attenuation and discontinuous synthesis during vesicular stomatitis virus transcription. Cell **23:**477-484.
42. **Ferron F, Longhi S, Henrissat B, Canard B.** 2002. Viral RNA-polymerases -- a predicted 2'-O-ribose methyltransferase domain shared by all Mononegavirales. Trends Biochem Sci **27:**222-224.
43. **Bailey TL, Boden M, Buske FA, Frith M, Grant CE, Clementi L, Ren J, Li WW, Noble WS.** 2009. MEME SUITE: tools for motif discovery and searching. Nucleic Acids Res **37:**W202-208.
44. **Lorenz R, Bernhart SH, Honer Zu Siederdissen C, Tafer H, Flamm C, Stadler PF, Hofacker IL.** 2011. ViennaRNA Package 2.0. Algorithms Mol Biol **6:**26.
45. **Miller WA, Giedroc D.** 2010. Ribosomal frameshifting in decoding plant viral RNAs, p 193–220. *In* Atkins JF, Gesteland RF (ed), Recoding: expansion of decoding rules enriches gene expression. Springer, New York.
46. **Walker PJ, Firth C, Widen SG, Blasdell KR, Guzman H, Wood TG, Paradkar PN, Holmes EC, Tesh RB, Vasilakis N.** 2015. Evolution of genome size and complexity in the *Rhabdoviridae*. PLoS Pathog **11:**e1004664.

47. **Lewis SH, Quarles KA, Yang Y, Tanguy M, Frezal L, Smith SA, Sharma PP, Cordaux R, Gilbert C, Giraud I, Collins DH, Zamore PD, Miska EA, Sarkies P, Jiggins FM.** 2018. Pan-arthropod analysis reveals somatic piRNAs as an ancestral defence against transposable elements. Nat Ecol Evol **2:**174-181.
48. **Suzuki Y, Frangeul L, Dickson LB, Blanc H, Verdier Y, Vinh J, Lambrechts L, Saleh MC.** 2017. Uncovering the repertoire of endogenous flaviviral elements in *Aedes* mosquito genomes. J Virol **91**.
49. **McBride CS, Baier F, Omondi AB, Spitzer SA, Lutomiah J, Sang R, Ignell R, Vosshall LB.** 2014. Evolution of mosquito preference for humans linked to an odorant receptor. Nature **515:**222-227.
50. **Bonizzoni M, Dunn WA, Campbell CL, Olson KE, Marinotti O, James AA.** 2012. Complex modulation of the *Aedes aegypti* transcriptome in response to dengue virus infection. PLoS One **7:**e50512.
51. **Bonizzoni M, Dunn WA, Campbell CL, Olson KE, Marinotti O, James AA.** 2012. Strain variation in the transcriptome of the dengue fever vector, *Aedes aegypti*. G3 **2:**103-114.
52. **Faucon F, Gaude T, Dusfour I, Navratil V, Corbel V, Juntarajumnong W, Girod R, Poupardin R, Boyer F, Reynaud S, David JP.** 2017. In the hunt for genomic markers of metabolic resistance to pyrethroids in the mosquito *Aedes aegypti*: An integrated next-generation sequencing approach. PLoS Negl Trop Dis **11:**e0005526.
53. **Alfonso-Parra C, Ahmed-Braimah YH, Degner EC, Avila FW, Villarreal SM, Pleiss JA, Wolfner MF, Harrington LC.** 2016. Mating-induced transcriptome changes in the reproductive tract of female *Aedes aegypti*. PLoS Negl Trop Dis **10:**e0004451.
54. **Sutton ER, Yu Y, Shimeld SM, White-Cooper H, Alphey AL.** 2016. Identification of genes for engineering the male germline of *Aedes aegypti* and *Ceratitis capitata*. BMC Genomics **17:**948.
55. **David JP, Faucon F, Chandor-Proust A, Poupardin R, Riaz MA, Bonin A, Navratil V, Reynaud S.** 2014. Comparative analysis of response to selection with three insecticides in the dengue mosquito *Aedes aegypti* using mRNA sequencing. BMC Genomics **15:**174.
56. **Metsky HC, Matranga CB, Wohl S, Schaffner SF, Freije CA, Winnicki SM, West K, Qu J, Baniecki ML, Gladden-Young A, Lin AE, Tomkins-Tinch CH, Ye SH, Park DJ, Luo CY, Barnes KG, Shah RR, Chak B, Barbosa-Lima G, Delatorre E, Vieira YR, Paul LM, Tan AL, Barcellona CM, Porcelli MC, Vasquez C, Cannons AC, Cone MR, Hogan KN, Kopp EW, Anzinger JJ, Garcia KF, Parham LA, Ramirez RMG, Montoya MCM, Rojas DP, Brown CM, Hennigan S, Sabina B, Scotland S, Gangavarapu K, Grubaugh ND, Oliveira G, Robles-Sikisaka R, Rambaut A, Gehrke L, Smole S, Halloran ME, Villar L, Mattar S, Lorenzana I, Cerbino-Neto J, Valim C, Degrave W, Bozza PT, Gnirke A, Andersen KG, Isern S, Michael SF, Bozza FA, Souza TML, Bosch I, Yozwiak NL, MacInnis BL, Sabeti PC.** 2017. Zika virus evolution and spread in the Americas. Nature **546:**411-415.
57. **Singh K.** 1967. Cell cultures derived from larvae of *Aedes albopictus* (Skuse) and *Aedes aegypti* (L.). Curr Sci **36:**506-508.
58. **Powell JR, Tabachnick WJ.** 2013. History of domestication and spread of *Aedes aegypti*--a review. Mem Inst Oswaldo Cruz **108 Suppl 1:**11-17.
59. **Brown JE, Evans BR, Zheng W, Obas V, Barrera-Martinez L, Egizi A, Zhao H, Caccone A, Powell JR.** 2014. Human impacts have shaped historical and recent evolution in *Aedes aegypti*, the dengue and yellow fever mosquito. Evolution **68:**514-525.

752 60. **Gloria-Soria A, Ayala D, Bheecarry A, Calderon-Arguedas O, Chadee DD,**
753 **Chiappero M, Coetzee M, Elahee KB, Fernandez-Salas I, Kamal HA, Kamgang**
754 **B, Khater EI, Kramer LD, Kramer V, Lopez-Solis A, Lutomiah J, Martins A, Jr.,**
755 **Micieli MV, Paupy C, Ponlawat A, Rahola N, Rasheed SB, Richardson JB, Saleh**
756 **AA, Sanchez-Casas RM, Seixas G, Sousa CA, Tabachnick WJ, Troyo A, Powell**
757 **JR.** 2016. Global genetic diversity of *Aedes aegypti*. Mol Ecol **25:**5377-5395.
758 61. **Suzuki Y, Frangeul L, Dickson LB, Blanc H, Verdier Y, Vinh J, Lambrechts L,**
759 **Saleh MC.** 2017. Uncovering the repertoire of endogenous flaviviral elements in
760 *Aedes* mosquito genomes. J Virol **91:**e00571-00517.
761 62. **Whitfield ZJ, Dolan PT, Kunitomi M, Tassetto M, Seetin MG, Oh S, Heiner C,**
762 **Paxinos E, Andino R.** 2017. The diversity, structure, and function of heritable
763 adaptive immunity sequences in the *Aedes aegypti* genome. Curr Biol **27:**3511-3519
764 e3517.
765 63. **Vodovar N, Bronkhorst A, van Cleef K, Miesen P, Blanc H, van Rij R, MC S.** 2012.
766 Arbovirus-derived piRNAs exhibit a ping-pong signature in mosquito cells. PLoS One
767 **7:**e30861.
768 64. **Brackney DE, Scott JC, Sagawa F, Woodward JE, Miller NA, Schilkey FD,**
769 **Mudge J, Wilusz J, Olson KE, Blair CD, Ebel GD.** 2010. C6/36 *Aedes albopictus*
770 cells have a dysfunctional antiviral RNA interference response. PLoS Neglect Trop
771 Dis **4:**e856.
772 65. **Léger P, Lara E, Jagla B, Sismeiro O, Mansuroglu Z, Coppée J, Bonnefoy E,**
773 **Bouloy M.** 2013. Dicer-2- and Piwi-mediated RNA interference in Rift Valley fever
774 virus-infected mosquito cells. J Virol **87:**1631-1648.
775 66. **Asad S, Parry R, Asgari S.** 2017. Upregulation of *Aedes aegypti Vago1* by
776 *Wolbachia* and its effect on dengue virus replication. Insect Biochem Mol Biol **92:**45-
777 52.
778 67. **Miesen P, Joosten J, van Rij RP.** 2016. PIWIs go viral: Arbovirus-derived piRNAs
779 in vector mosquitoes. PLoS Pathog **12:**e1006017.
780 68. **Di Giallonardo F, Audsley MD, Shi M, Young PR, McGraw EA, Holmes EC.** 2018.
781 Complete genome of *Aedes aegypti* anphevirus in the Aag2 mosquito cell line. J Gen
782 Virol **doi: 10.1099/jgv.0.001079**.
783 69. **Lee M, Etebari K, Hall-Mendelin S, van den Hurk AF, Hobson-Peters J, Vatipally**
784 **S, Schnettler E, Hall R, Asgari S.** 2017. Understanding the role of microRNAs in the
785 interaction of *Aedes aegypti* mosquitoes with an insect-specific flavivirus. J Gen Virol
786 **98:**1892-1903.
787 70. **Etebari K, Osei-Amo S, Blomberg SP, Asgari S.** 2015. Dengue virus infection
788 alters post-transcriptional modification of microRNAs in the mosquito vector *Aedes*
789 *aegypti*. Sci Rep **5:**15968.
790 71. **Kuno G.** 1983. Cultivation of mosquito cell lines in serum-free media and their effects
791 on dengue virus replication. In Vitro **19:**707-713.
792 72. **O'Neill SL, Kittayapong P, Braig HR, Andreadis TG, Gonzalez JP, Tesh RB.**
793 1995. Insect densoviruses may be widespread in mosquito cell lines. J Gen Virol **76**
794 **(Pt 8):**2067-2074.
795 73. **Juliano SA, Lounibos LP, O'Meara GF.** 2004. A field test for competitive effects of
796 *Aedes albopictus* on *A. aegypti* in South Florida: differences between sites of
797 coexistence and exclusion? Oecologia **139:**583-593.
798 74. **Blair C, Olson K.** 2015. The role of RNA interference (RNAi) in arbovirus-vector
799 interactions. Viruses **7:**820-843.
800 75. **Hussain M, Etebari K, Asgari S.** 2016. Functions of small RNAs in mosquitoes. Adv
801 Insect Physiol **51:**189-222.

802 76. **Schnettler E, Donald CL, Human S, Watson M, Siu RW, McFarlane M, Fazakerley**
803 **JK, Kohl A, Fragkoudis R.** 2013. Knockdown of piRNA pathway proteins results in
804 enhanced Semliki Forest virus production in mosquito cells. J Gen Virol **94:**1680-
805 1689.
806 77. **Dietrich I, Shi X, McFarlane M, Watson M, Blomstrom AL, Skelton JK, Kohl A,**
807 **Elliott RM, Schnettler E.** 2017. The antiviral RNAi response in vector and non-vector
808 cells against Orthobunyaviruses. PLoS Negl Trop Dis **11:**e0005272.
809 78. **Hess AM, Prasad AN, Ptitsyn A, Ebel GD, Olson EN, Barbacioru C, Monighetti**
810 **C, Campbell CL.** 2011. Small RNA profiling of Dengue virus-mosquito interactions
811 implicates the PIWI RNA pathway in anti-viral defense. BMC Microbiol **11:**45.
812 79. **Varjak M, Donald CL, Mottram TJ, Sreenu VB, Merits A, Maringer K, Schnettler**
813 **E, Kohl A.** 2017. Characterization of the Zika virus induced small RNA response in
814 *Aedes aegypti* cells. PLoS Negl Trop Dis **11:**e0006010.
815 80. **Saldaña MA, Etebari K, Hart CE, Widen SG, Wood TG, Thangamani S, Asgari S,**
816 **Hughes GL.** 2017. Zika virus alters the microRNA expression profile and elicits an
817 RNAi response in *Aedes aegypti* mosquitoes. PLoS Neg Trop Dis **11:**e0005760.
818 81. **Lee M, Etebari K, Hall-Mendelin S, van den Hurk AF, Hobson-Peters J, Vatipally**
819 **S, Schnettler E, Hall R, Asgari S.** 2017. Understanding the role of microRNAs in the
820 interaction of *Aedes aegypti* mosquitoes with an insect-specific flavivirus. J Gen Virol
821 **98:**892-1903.
822 82. **Johnson KN.** 2015. The impact of *Wolbachia* on virus infection in mosquitoes.
823 Viruses **7:**5705-5717.
824 83. **Schultz MJ, Tan AL, Gray CN, Isern S, Michael SF, Frydman HM, Connor JH.**
825 2018. *Wolbachia w*Stri blocks Zika virus growth at two independent stages of viral
826 replication. MBio **9:**e00738-00718.
827 84. **Dodson BL, Andrews ES, Turell MJ, Rasgon JL.** 2017. *Wolbachia* effects on Rift
828 Valley fever virus infection in *Culex tarsalis* mosquitoes. PLoS Negl Trop Dis
829 **11:**e0006050.
830 85. **Hornak KE, Lanchy JM, Lodmell JS.** 2016. RNA encapsidation and packaging in
831 the phleboviruses. Viruses **8:**E194.
832 86. **Raymond DD, Piper ME, Gerrard SR, Skiniotis G, Smith JL.** 2012. Phleboviruses
833 encapsidate their genomes by sequestering RNA bases. Proc Natl Acad Sci U S A
834 **109:**19208-19213.
835 87. **Choi KH.** 2012. Viral polymerases. Adv Exp Med Biol **726:**267-304.
836 88. **Harak C, Lohmann V.** 2015. Ultrastructure of the replication sites of positive-strand
837 RNA viruses. Virology **479-480:**418-433.
838 89. **Rainey SM, Martinez J, McFarlane M, Juneja P, Sarkies P, Lulla A, Schnettler E,**
839 **Varjak M, Merits A, Miska EA, Jiggins FM, Kohl A.** 2016. *Wolbachia* blocks viral
840 genome replication early in infection without a transcriptional response by the
841 endosymbiont or host small RNA pathways. PLoS Pathog **12:**e1005536.
842 90. **Schultz MJ, Isern S, Michael SF, Corley RB, Connor JH, Frydman HM.** 2017.
843 Variable inhibition of Zika virus replication by different *Wolbachia* strains in mosquito
844 cell cultures. J Virol **91:**e00339-00317.
845 91. **Pan X, Pike A, Joshi D, Bian G, McFadden MJ, Lu P, Liang X, Zhang F, Raikhel**
846 **AS, Xi Z.** 2018. The bacterium *Wolbachia* exploits host innate immunity to establish
847 a symbiotic relationship with the dengue vector mosquito *Aedes aegypti*. ISME J
848 **12:**277-288.
849 92. **Rice DW, Sheehan KB, Newton ILG.** 2017. Large-scale identification of *Wolbachia*
850 *pipientis* effectors. Genome Biol Evol **9:**1925-1937.

93. **Amuzu HE, Tsyganov K, Koh C, Herbert RI, Powell DR, McGraw EA.** 2018. *Wolbachia* enhances insect-specific flavivirus infection in *Aedes aegypti* mosquitoes. J Gen Virol **DOI: 10.1002/ece3.4066**.
94. **Karpf AR, Lenches E, Strauss EG, Strauss JH, Brown DT.** 1997. Superinfection exclusion of alphaviruses in three mosquito cell lines persistently infected with Sindbis virus. J Virol **71:**7119-7123.
95. **Pudney M, Varma M, Leake C.** 1979. Establishment of cell lines from larvae of culicine (*Aedes* species) and anopheline mosquitoes. TCA Mannual **5:**997-1002.
96. **Ladner JT, Beitzel B, Chain PS, Davenport MG, Donaldson EF, Frieman M, Kugelman JR, Kuhn JH, O'Rear J, Sabeti PC, Wentworth DE, Wiley MR, Yu GY, Threat Characterization C, Sozhamannan S, Bradburne C, Palacios G.** 2014. Standards for sequencing viral genomes in the era of high-throughput sequencing. MBio **5:**e01360-01314.
97. **Hussain M, Frentiu FD, Moreira LA, O'Neill SL, Asgari S.** 2011. *Wolbachia* uses host microRNAs to manipulate host gene expression and facilitate colonization of the dengue vector *Aedes aegypti*. Proc Natl Acad Sci U S A **108:**9250-9255.
98. **Zimmermann L, Stephens A, Nam SZ, Rau D, Kubler J, Lozajic M, Gabler F, Soding J, Lupas AN, Alva V.** 2017. A completely reimplemented MPI bioinformatics toolkit with a new HHpred server at its core. J Mol Biol **doi: 10.1016/j.jmb.2017.12.007**.
99. **Tsirigos KD, Peters C, Shu N, Kall L, Elofsson A.** 2015. The TOPCONS web server for consensus prediction of membrane protein topology and signal peptides. Nucleic Acids Res **43:**W401-407.

Figure legends:

Figure 1. Presence of Aedes anphevirus (AeAV) in insect cell lines, and genome organisation and phylogeny of the virus. A) RT-PCR analysis of *Aedes* cell lines Aag2, Aag2.*w*MelPop-CLA (Pop), *w*MelPop-CLA.Tet (Pop-T), Aa20, RML-12, and C6/36 for the presence of AeAV. RPS17 was used as a loading control. **B)** Genome organisation of the Cali, Colombia AeAV genome strain and subgenomic gene transcription profile. Transmembrane domains (TMD) are depicted as boxes with dashed lines and signal peptide is depicted as a blue box. NP, nucleoprotein; G, glycoprotein; ZnF, zinc-like finger; RdRP, RNA dependent RNA polymerase. **C)** AeAV is a member of the *Anphevirus* genus (red), related to members of the *Nyamiviridae* (pink) and *Bornaviridae* (purple) in an unassigned family within the order *Mononegavirales*. A multiple sequence alignment of the RNA dependent RNA polymerase and the mRNA capping domain was used to create a Maximum likelihood phylogeny. The phylogeny is arbitrarily rooted. 1000 bootstraps were performed and branches with bootstrap values greater than 85% are highlighted. Branch length

888 represent expected numbers of substitutions per amino acid site. Genbank protein
889 accession numbers are Bolahun virus variant 1 (AOR51366.1), Culex mononega-like virus
890 1 (CMLV1) (ASA47369.1), Culex mononega-like virus 2 (CMLV2) (ASA47322.1), Gambie
891 virus (AOR51379.1), Xincheng Mosquito Virus (XcMV) (YP_009302387.1), Borna disease
892 virus (YP_009269418.1), Canary bornavirus 1 (YP_009268910.1), Loveridges garter snake
893 virus 1 (YP_009055063.1), Parrot bornavirus 1 (AEG78314.1), Variegated squirrel
894 bornavirus 1 (SBT82903.1), Midway nyavirus (YP_002905331.1), Nyamanini nyavirus
895 (YP_002905337.1), Sierra Nevada virus (YP_009044201.1), Soybean cyst nematode
896 socyvirus (YP_009052467.1), Farmington virus (YP_009091823.1), Beihai rhabdo-like virus
897 3 (APG78650.1), Beihai rhabdo-like virus 5 (YP_009333422.1), Beihai rhabdo-like virus 6
898 (YP_009333413.1), Drosophila unispina virus 1 (AMK09260.1), Hubei diptera virus 11
899 (YP_009337182.1), Hubei orthoptera virus 5 (YP_009336728.1), Hubei rhabdo-like virus 7
900 (YP_009337121.1), Orinoco virus (ANQ45640.1), Sanxia Water Strider Virus 4
901 (YP_009288955.1), Shuangao Fly Virus 2 (AJG39135.1), Wenling crustacean virus 12
902 (YP_009336618.1), Wenzhou Crab Virus 1 (YP_009304558.1), Wenzhou tapeworm virus 1
903 (YP_009342311.1), Wuchan romanomermis nematode virus 2 (YP_009342285.1).
904 **Figure 2: Conservation of GATA-like Zinc finger (ZnF) domain and small transmembrane**
905 **domain containing protein between tentative members of the *Anphevirus* taxon. A)** Genome
906 orientation of previously discovered viruses within the *Anphevirus* taxon, and **B)** two viruses within
907 a closely related clade. Predicted ORF encoding the ZnF domain is indicated by a black square.
908 Predicted ORFs containing transmembrane domains are indicated by dashed lines. Genbank
909 accession numbers are shown below virus name. NP, nucleoprotein; G, glycoprotein; ZnF, zinc-
910 like finger; RdRP, RNA dependent RNA polymerase. **C)** Alignment of predicted GATA-like ZnF
911 protein sequence (C-X(2)-C-X(17-20)-C-X(2)-C) between three representative strains of AeAV
912 (Miami, USA ; Pune, India; Rabai, Kenya) and predicted ZnF domain proteins from Figure 2A and
913 B.

914 **Figure 3. Aedes anphevirus (AeAV) *cis*-regulatory elements. A)** Location and orientation of
915 predicted *cis*-regulatory element in AeAV indicated by numbered red arrows; downwards indicating
916 genome and upwards arrow indicating anti-genome. **B)** Predicted minimum free energy (MFE) RNA
917 structure of the region surrounding the motif for each element using the RNAfold web server. Colour
918 indicates probability of base-pairing and motif is indicated by the black line. **C)** Sequence of the
919 conserved motif as predicted by MEME as well as location and the statistical confidence of the motif.
920 Sequences are written 3' to 5' and anti-genome motif sequences 1 and 7 are depicted as reverse
921 complement for visual clarity.

922 **Figure 4. Aedes anphevirus (AeAV) has worldwide distribution in *Ae. aegypti* laboratory**
923 **colonies, cell lines and wild-caught mosquitoes.** Locations of mosquito collection from RNA-
924 Seq data that were positive for AeAV (Table S1). Points refer to collection sites from American
925 (orange), Asia-Pacific (blue) and African (green) locations.

926 **Figure 5. Aedes anphevirus (AeAV) strains have evolved into African, Asia-Pacific and**
927 **American lineages. A)** Maximum likelihood phylogeny (PhyML) between AeAV strains using a
928 General Time Reversible (GTR) + G +T model with 1000 bootstraps. Branch lengths represent
929 expected numbers of substitutions per nucleotide site. For visual clarity, the RML-12 clade and Miami
930 clades were collapsed and single examples were shown. **B)** Evolutionary history of worldwide
931 sampling of *Ae. aegypti* adapted from (59, 60) from 1504 SNPs species. Bootstrapped neighbour-
932 joining network based on population pairwise chord-distances from with node support over 90% is
933 shown on relevant branches. New World (American) populations in yellow, and Asia-Pacific
934 populations are shown in light blue. We have truncated the tree and rooted to the *Ae. aegypti*
935 *formosus* (Aef) shown as a red branch.

936 **Figure 6. Genomic context for anphevirus-like insertions into the *Ae. aegypti* genome.** A 21,
937 242nt portion of chromosome 2 depicting anphevirus insertions (red) with predicted ORFs that
938 encode for LTR retrotransposase elements (yellow).

939 **Figure 7. Aedes anphevirus (AeAV) is infectious to *Aedes* cell lines but does not replicate in**
940 **Huh-7, Vero and BSR vertebrate cell lines. (A)** RT-qPCR of AeAV genome and anti-genome in a
941 five-day time course in *Ae. aegypti* Aa20 cells, and *Ae. albopictus* C6/36 cells. Error bars represent
942 the SEM of three biological replicates. **(B)** RT-PCR of AeAV genome in a seven-day time course in
943 Human hepatocellular carcinoma cells (Huh-7)**,** African green monkey cells (Vero), Baby Hamster
944 Kidney (BSR). M, Mock infected cells.

945 **Figure 8. Aedes anphevirus (AeAV) genome replication is enhanced by *Wolbachia* infection**
946 **in *Ae. aegypti* cells and produces abundant vsiRNAs and vpiRNAs. A)** RT-qPCR of the AeAV
947 genomic (gRNA) and antigenomic RNA in tetracycline cured Aag2.*w*MelPop-CLA cells (Pop-tet) and
948 Aag2.*w*MelPop-CLA cells (Pop) relative to RPS17. Error bars represent the SEM of six (genome)
949 and three (antigenome) biological replicates. n.s, not significant; **, $p < 0.01$. **B)** Mapping profile of
950 pooled small RNA fraction in Aag2.*w*MelPop-CLA cells. **C)** Alignment of the 21-nt sRNA reads
951 (representing siRNAs), and **D)** the 26-31nt reads (representing piRNAs) mapped to the AeAV
952 antigenome (blue) and genome (red) in Aag2.*w*MelPop-CLA cells. Relative nucleotide frequency
953 and conservation of the 28nt small RNA reads that mapped to the **E)** genome, and the **F)** anti-
954 genome of AeAV in Aag2.*w*MelPop-CLA cells.

955 **Figure 9. Aedes anphevirus (AeAV) reduces dengue virus replication in Aa20 cells.** Aa20 cells
956 persistently infected with AeAV were infected with **(A)** 0.1 and **(B)** 1 MOI of dengue virus serotype 2
957 (DENV-2). Total RNA was extracted at 0, 1, 3 and 5 days following DENV-2 inoculation and analysed
958 by RT-qPCR. **(C)** RT-qPCR analysis of AeAV persistently infected Aa20 cells infected with 0.1 and
959 1 MOI of DENV-2 using specific primers to the AeAV genome. Error bars represent the SEM of three
960 biological replicates. n.s, not significant; *, $p < 0.05$; **, $p < 0.01$.

961 **Figure 10. Aedes anphevirus (AeAV) is potentially vertically transmitted. A)** Diagram showing
962 the parental (K14, K27) and hybrid strains (GP1, GP2, HP1, HP2) from (49). **B)** Table showing
963 assembly statistics and BLASTN similarity of AeAV assembled from K14 and K27 hybrid strains.

Figure 1

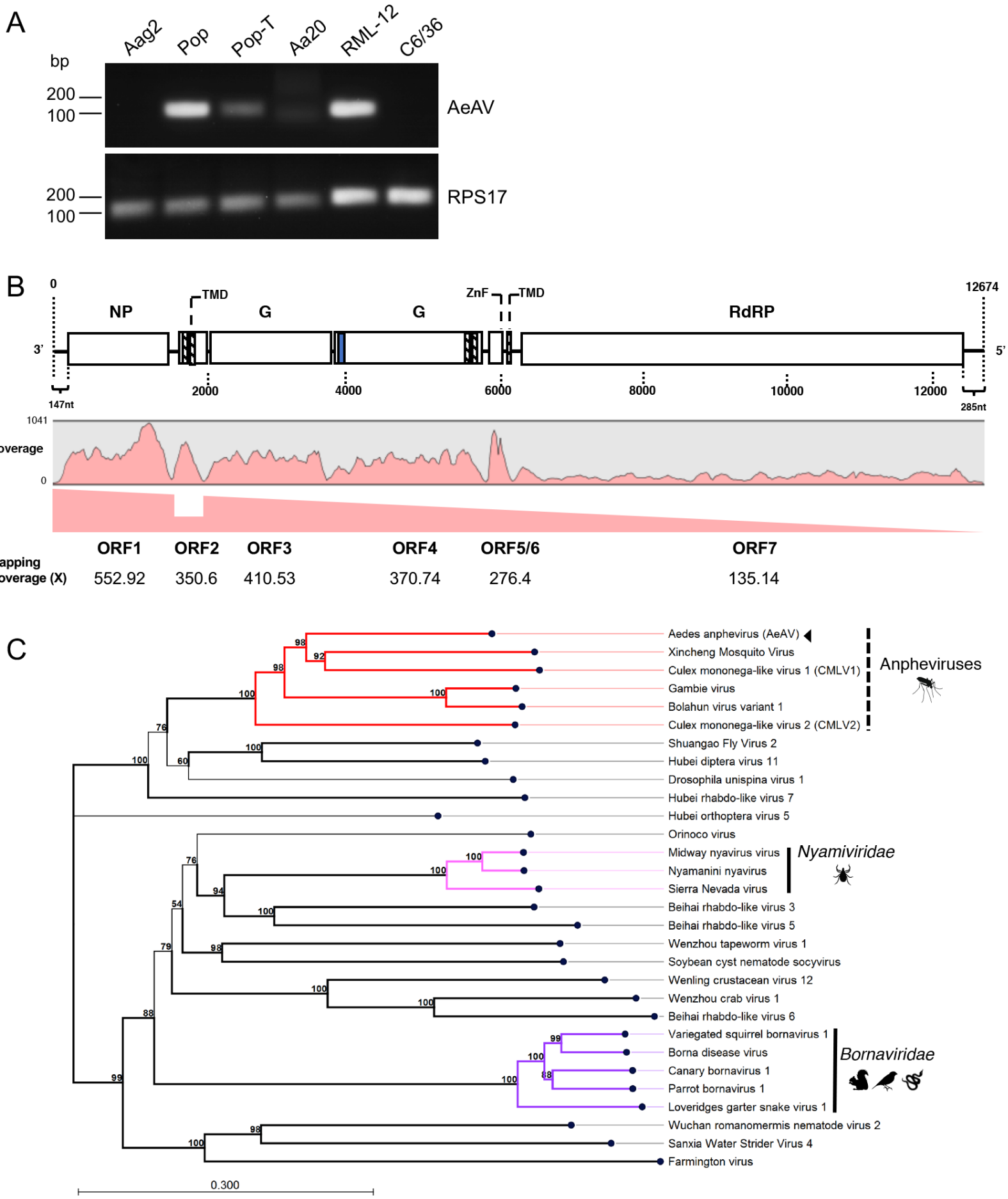
A
Aag2
Pop
Pop-T
Aa20
RML-12
C6/36
bp
200
100
AeAV
200
100
RPS17
B
0
NP
TMD
G
G
ZnF
TMD
RdRP
12674
3'
5'
2000
4000
6000
8000
10000
12000
147nt
285nt
1041
Coverage
0
ORF1
ORF2
ORF3
ORF4
ORF5/6
ORF7
Mapping Coverage (X)
552.92
350.6
410.53
370.74
276.4
135.14
C
Aedes anphevirus (AeAV)
Xincheng Mosquito Virus
Culex mononega-like virus 1 (CMLV1)
Gambie virus
Bolahun virus variant 1
Culex mononega-like virus 2 (CMLV2)
Anpheviruses
Shuangao Fly Virus 2
Hubei diptera virus 11
Drosophila unispina virus 1
Hubei rhabdo-like virus 7
Hubei orthoptera virus 5
Orinoco virus
Midway nyavirus virus
Nyamanini nyavirus
Sierra Nevada virus
Nyamiviridae
Beihai rhabdo-like virus 3
Beihai rhabdo-like virus 5
Wenzhou tapeworm virus 1
Soybean cyst nematode socyvirus
Wenling crustacean virus 12
Wenzhou crab virus 1
Beihai rhabdo-like virus 6
Variegated squirrel bornavirus 1
Borna disease virus
Canary bornavirus 1
Parrot bornavirus 1
Loveridges garter snake virus 1
Bornaviridae
Wuchan romanomermis nematode virus 2
Sanxia Water Strider Virus 4
Farmington virus
0.300

Figure 2

A

Xincheng Mosquito Virus, (XcMV) (KM817661.1)

Gambie virus, (KX148553.1)

Culex mononega-like virus 1 (CMLV-1) Segment 2 (MF176317.1)

Culex mononega-like virus 2 (CMLV-2), (MF176298.1)

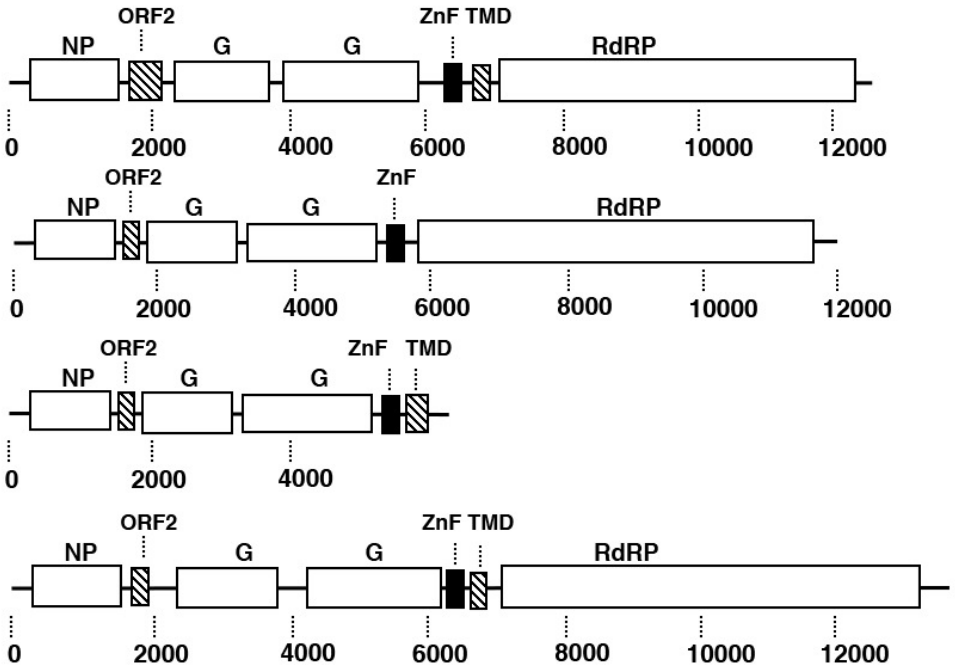

B

Hubei diptera virus 11, (KX884430.1)

Shuangao Fly Virus 2, Incomplete (KM817638.1)

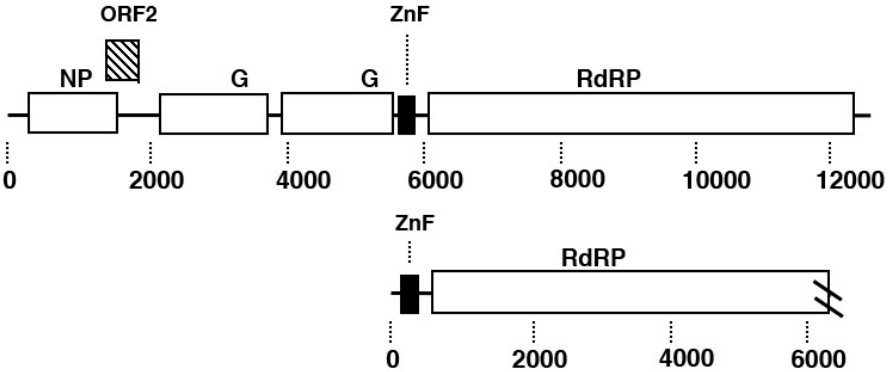

C

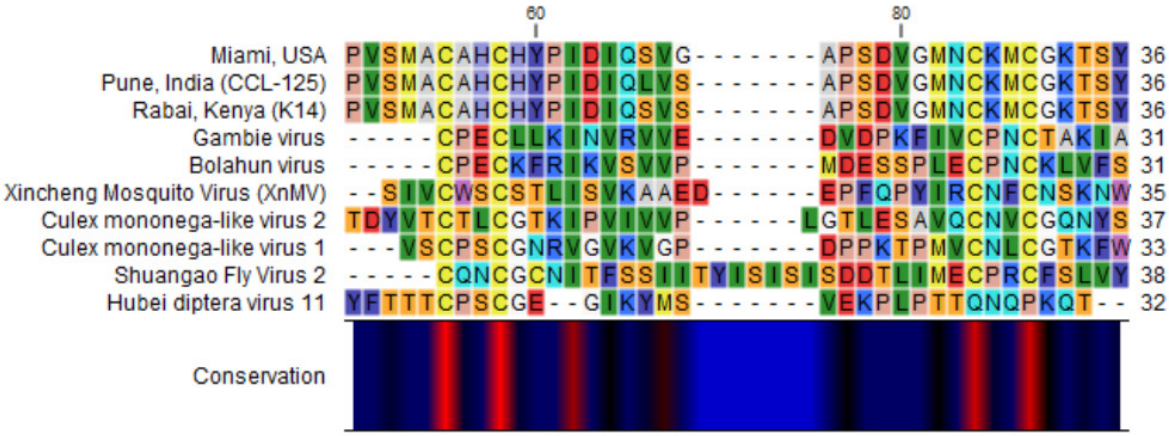

Figure 3

A

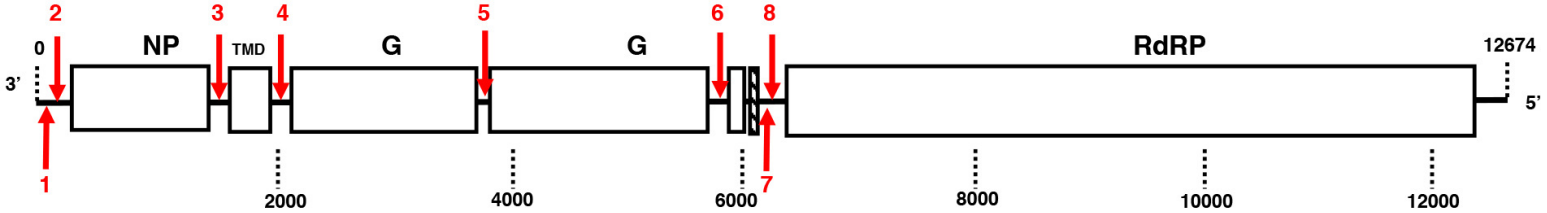

B

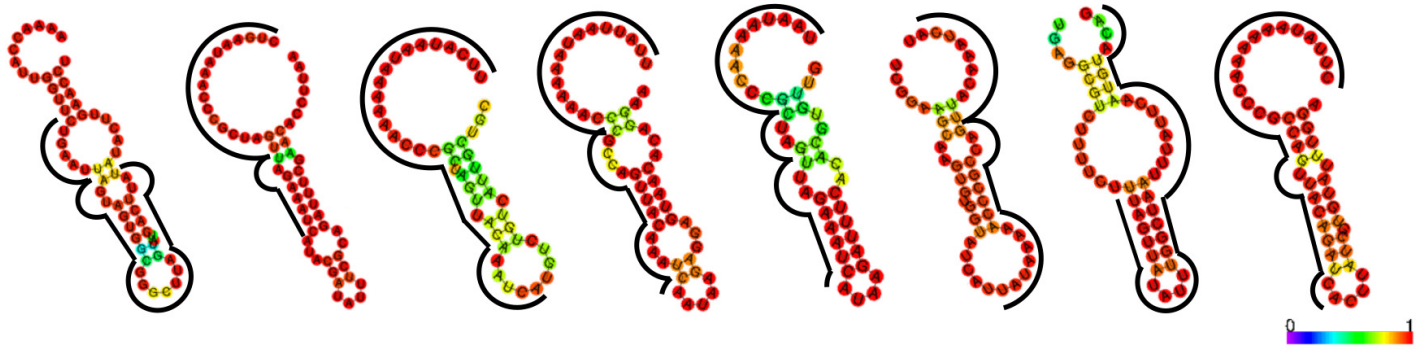

C

Element	Strand	Start	*p*-value	Motif	UUVCUHWUAAAAAACCCGCYAGUUASAAAUCA	
1	-	17	3.0e-5	AGUAUA	UAAGUGAUACUAAGCCCGCCACUACUAAUUCA	GAACCA
2	+	71	3.1e-16	ACGGUG	UUACUCUGAAUAAACCCGCUAGUUAGAAAUCA	UACGAU
3	+	1591	8.8e-18	CGAAAU	UUCAUAAUAAAAAACCCGCUAGUUACAAAUCA	UGUCUG
4	+	2048	2.3e-17	AUGUUU	UUAUUAAUAAAAAACCCGCCAGUUACAAAUCA	AUAAGA
5	+	3695	5.0e-16	AGCUAC	UCCCUUUAAUAAAACCCGCUAGUUAGAAAUCA	UAAGAU
6	+	5867	7.0e-11	GUGUGG	UAUCAUUAUAAAAACCCGCCAGUUACAAAUCA	UGCCUG
7	-	6178	7.3e-5	GAACCU	GUACAUUGAAUAAAUUAGCCAAAUAUAACUAA	AGAAAA
8	+	6218	5.3e-17	GUUCUC	UUGCUUAUAAAAAACCCGCCAGUUACAGAUCA	CUUAUC

Figure 4

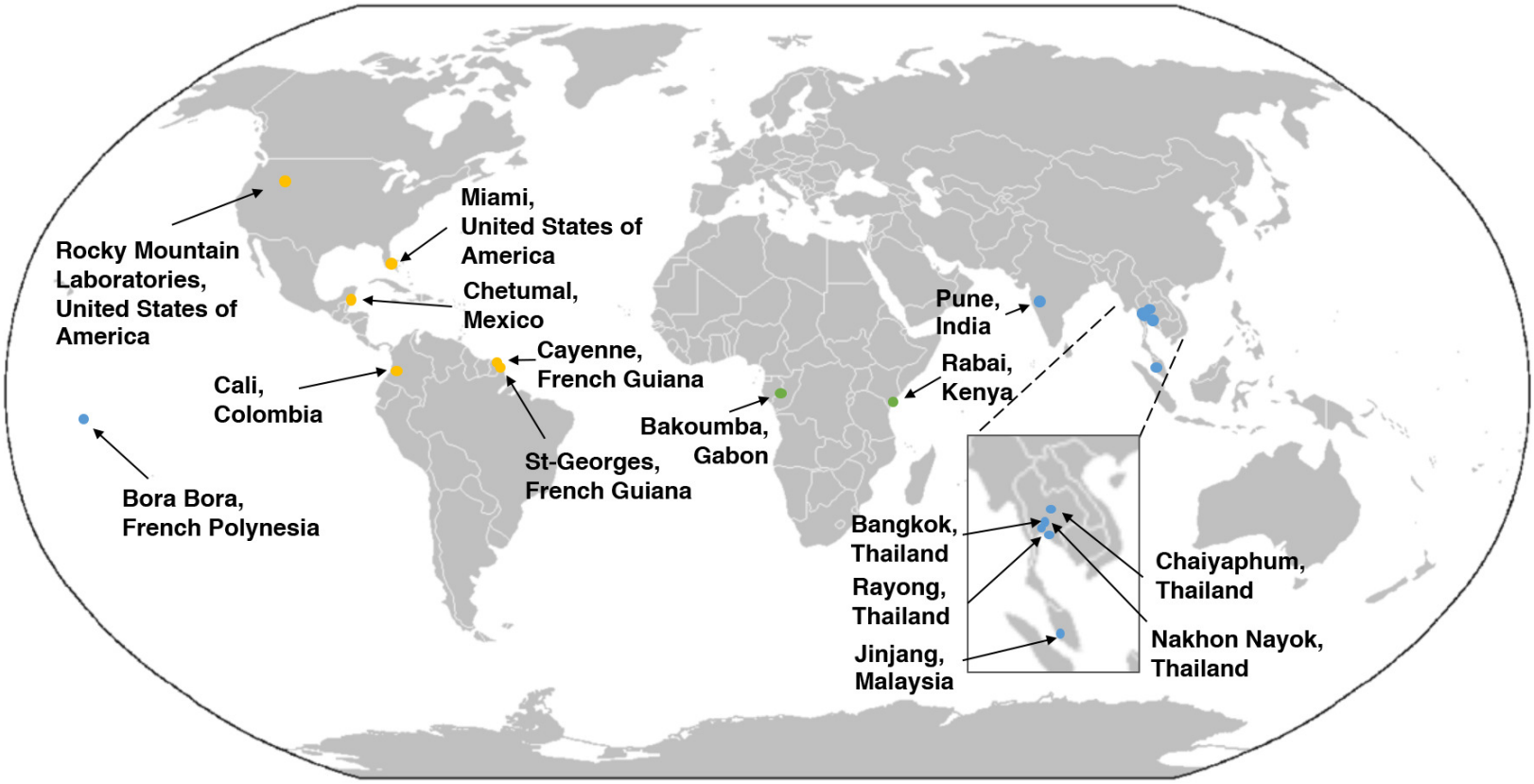
Rocky Mountain Laboratories, United States of America
Miami, United States of America
Chetumal, Mexico
Cayenne, French Guiana
Cali, Colombia
St-Georges, French Guiana
Bora Bora, French Polynesia
Bakoumba, Gabon
Pune, India
Rabai, Kenya
Bangkok, Thailand
Rayong, Thailand
Jinjang, Malaysia
Chaiyaphum, Thailand
Nakhon Nayok, Thailand

Figure 5

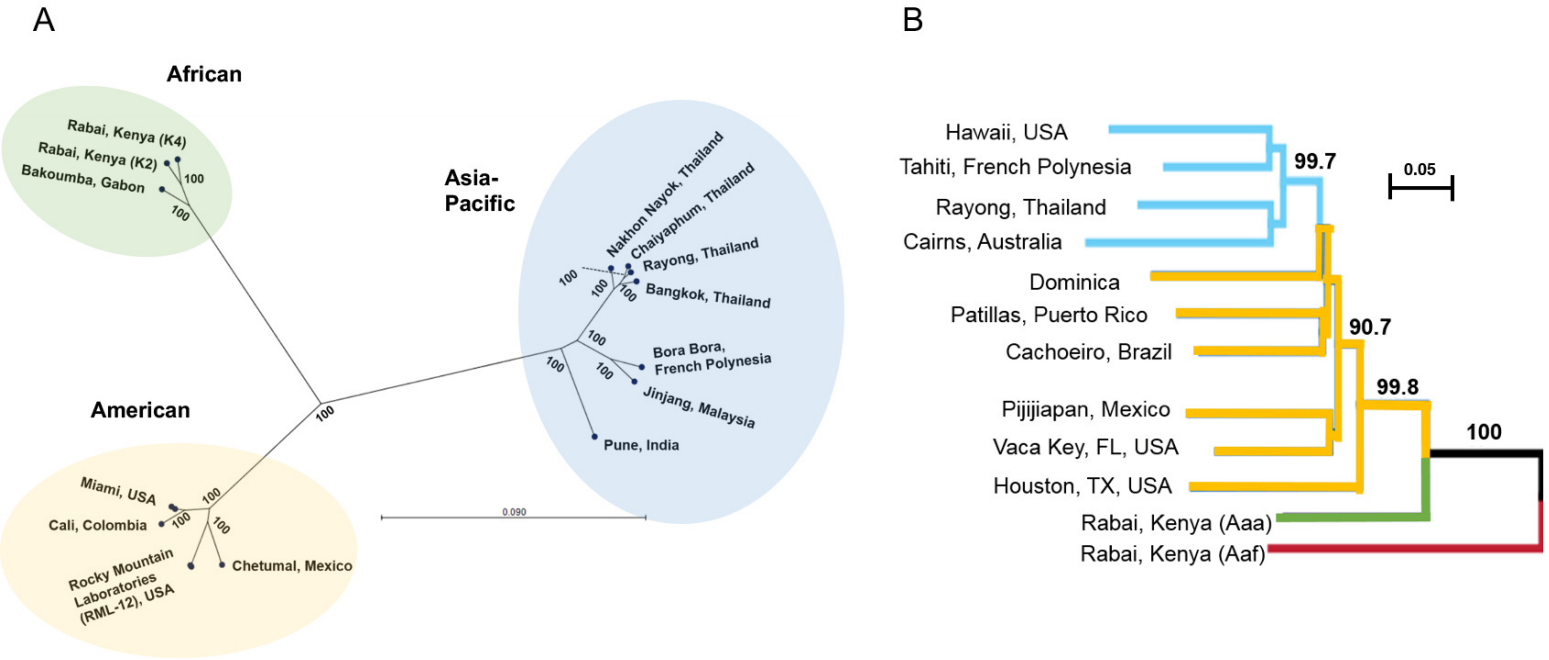
A
African
Rabai, Kenya (K4)
Rabai, Kenya (K2)
Bakoumba, Gabon
Asia-Pacific
Nakhon Nayok, Thailand
Chaiyaphum, Thailand
Rayong, Thailand
Bangkok, Thailand
Bora Bora, French Polynesia
Jinjang, Malaysia
Pune, India
American
Miami, USA
Cali, Colombia
Rocky Mountain Laboratories (RML-12), USA
Chetumal, Mexico
0.090
B
Hawaii, USA
Tahiti, French Polynesia
Rayong, Thailand
Cairns, Australia
Dominica
Patillas, Puerto Rico
Cachoeiro, Brazil
Pijijiapan, Mexico
Vaca Key, FL, USA
Houston, TX, USA
Rabai, Kenya (Aaa)
Rabai, Kenya (Aaf)
99.7
90.7
99.8
100
0.05

Figure 6

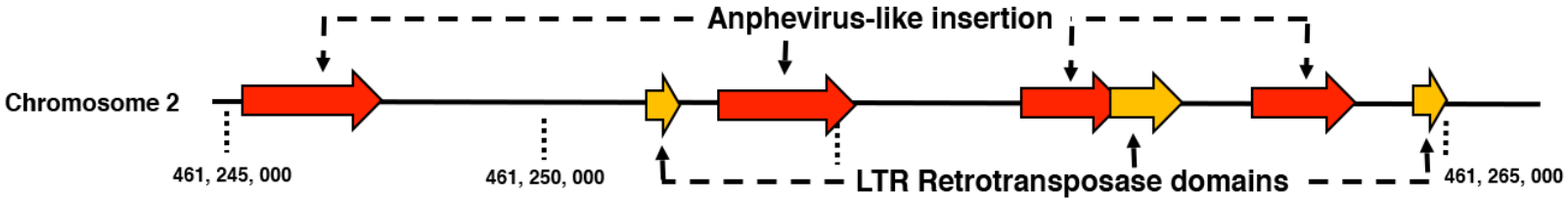
Anphevirus-like insertion
Chromosome 2
461, 245, 000
461, 250, 000
LTR Retrotransposase domains
461, 265, 000

Figure 7

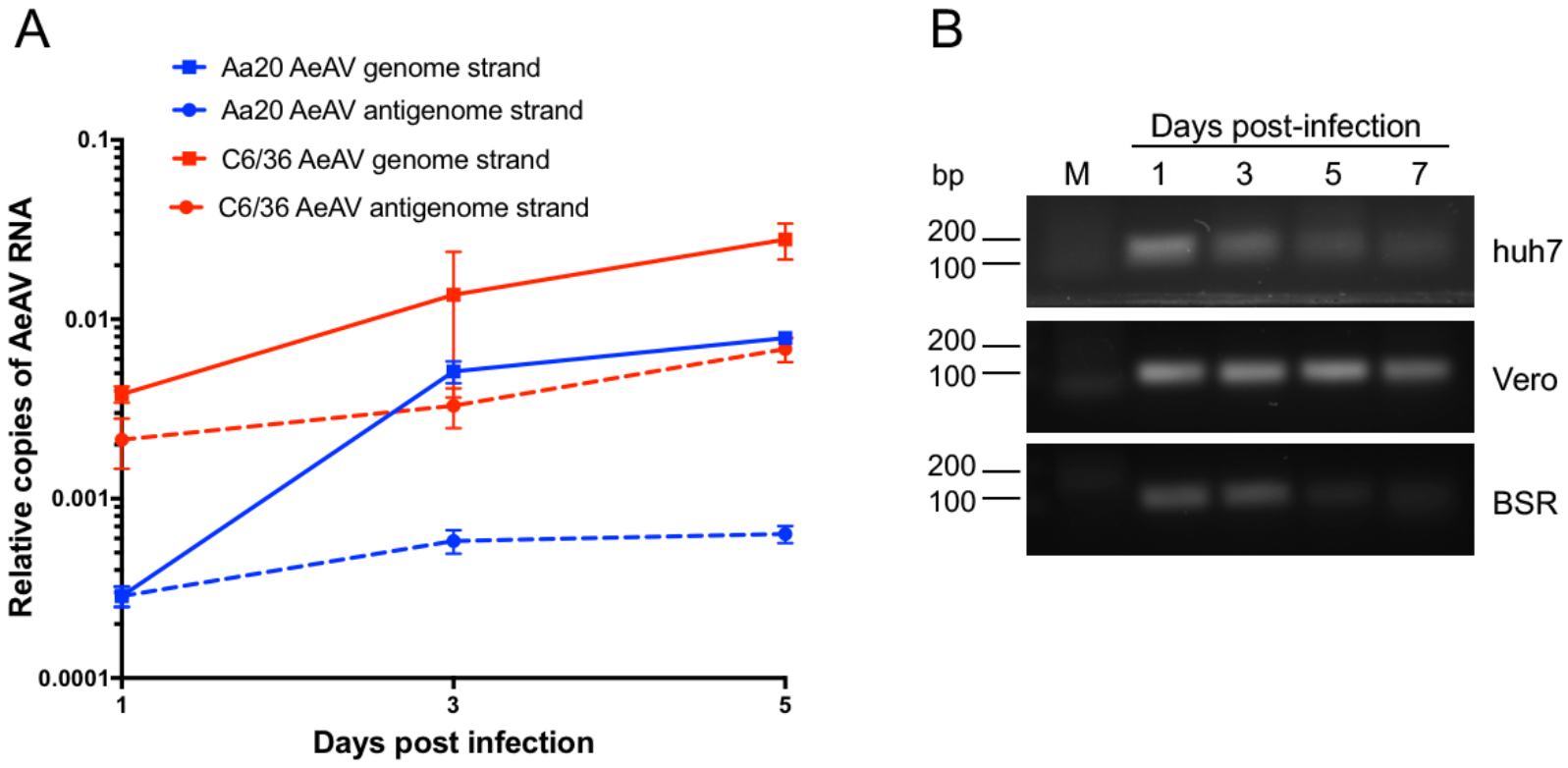
A
Aa20 AeAV genome strand
Aa20 AeAV antigenome strand
C6/36 AeAV genome strand
C6/36 AeAV antigenome strand
Relative copies of AeAV RNA
0.1
0.01
0.001
0.0001
1
3
5
Days post infection
B
Days post-infection
bp
M
1
3
5
7
200
100
huh7
Vero
BSR

Figure 8

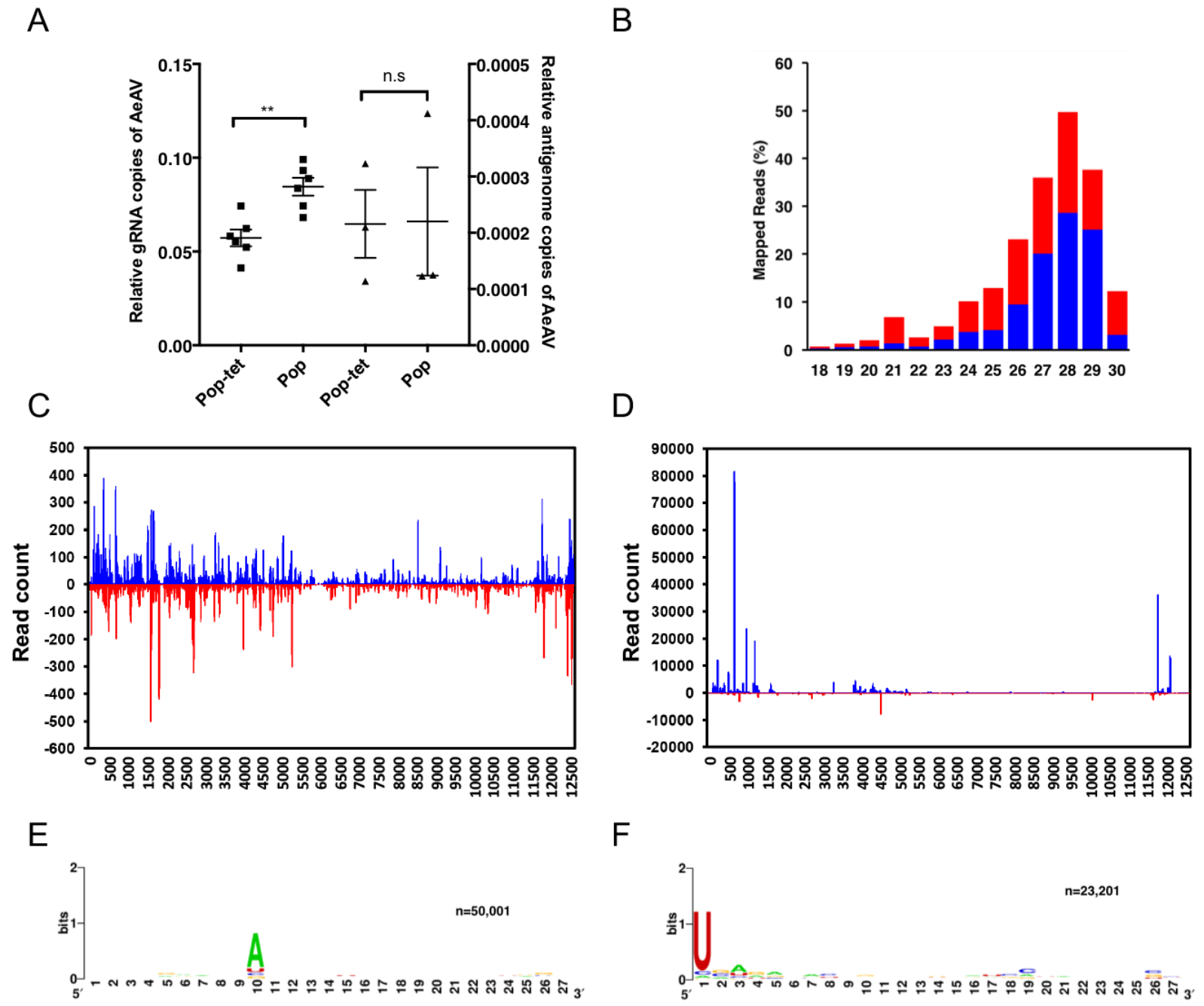
A
Relative gRNA copies of AeAV
Relative antigenome copies of AeAV
**
n.s
Pop-tet
Pop
Pop-tet
Pop
B
Mapped Reads (%)
C
Read count
D
Read count
E
bits
n=50,001
F
bits
n=23,201

Figure 9

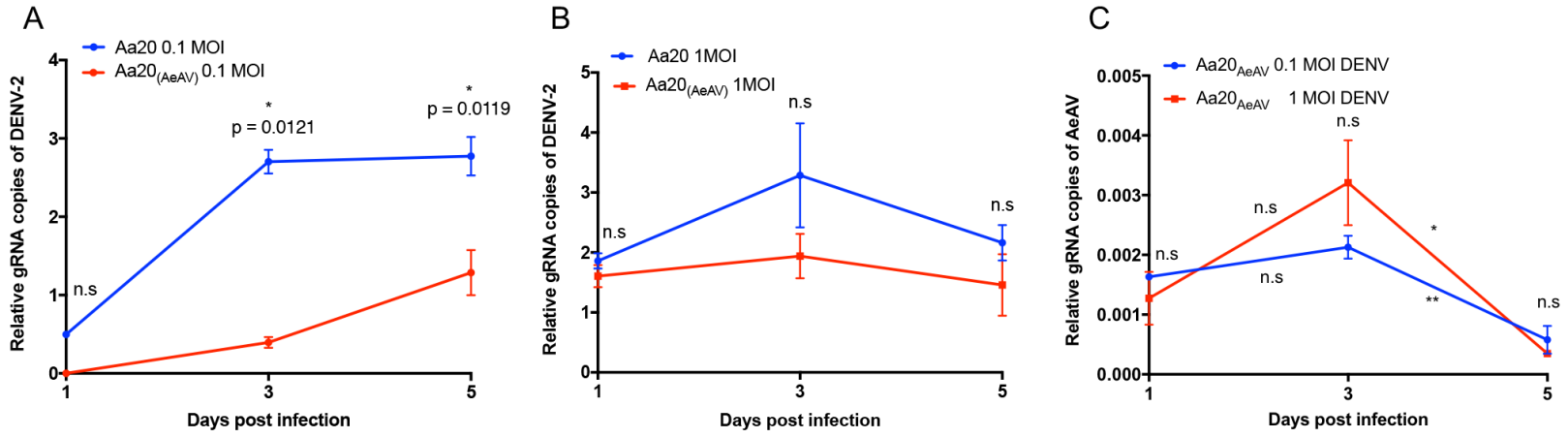
A
Aa20 0.1 MOI
Aa20(AeAV) 0.1 MOI
Relative gRNA copies of DENV-2
n.s
*
p = 0.0121
*
p = 0.0119
Days post infection
B
Aa20 1MOI
Aa20(AeAV) 1MOI
Relative gRNA copies of DENV-2
n.s
n.s
n.s
Days post infection
C
Aa20AeAV 0.1 MOI DENV
Aa20AeAV 1 MOI DENV
Relative gRNA copies of AeAV
n.s
n.s
n.s
n.s
*
**
n.s
Days post infection

Figure 10

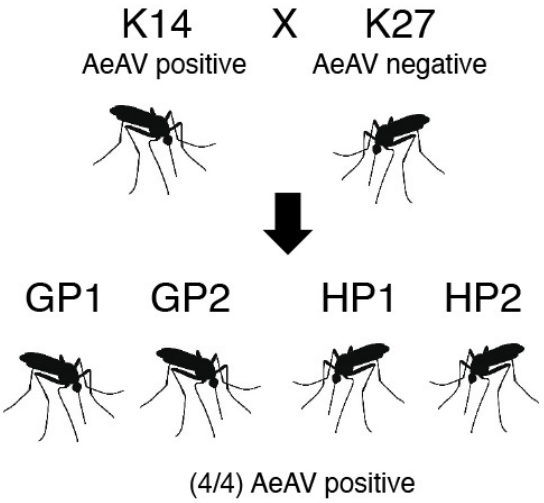

Parental Strains		K14	K27	
Assembled AeAV genome		13,012	-	
Hybrid Strains	**GP1**	**GP2**	**HP1**	**HP2**
Assembled AeAV genome	13,059	13,034	13,010	7,191; 5,962
BLASTN identity to K14	100%	100%	100%	100%